

The Basics of Loop Quantum Gravity

Discussion 4: Building Space & Time

International Society of
Quantum Gravity
June 28th, 2023

Hal M. Haggard,
Bard College

Review question 1: What are the conjugate variables that LQG uses in its gauge theory description of GR?

Review question 1: What are the conjugate variables that LQG uses in its gauge theory description of GR?

The gravitational electric field, $\tilde{E}_i^a = \sqrt{\det q} E_i^a$, and 2-form

$$E^i(x) = \tilde{E}^{ia}(x) \epsilon_{abc} dx^b \wedge dx^c.$$

The conjugate connection: $A_a^i := \Gamma_a^i + \gamma K_a^i$, with $\gamma \in \mathbb{R}$, $K_a^i = K_{ab} E^{bi}$, and $\Gamma_a^i = \frac{1}{2} \epsilon^i_{jk} \omega_a^{jk}$.

Then: $\{A_a^i(x), \tilde{E}_j^b(y)\} = \gamma \delta_j^i \delta_a^b \delta^{(3)}(x, y)$, $\{A, A\} = 0$, & $\{\tilde{E}, \tilde{E}\} = 0$.

Review question 2: Where was the cat hiding in quantum gravity?



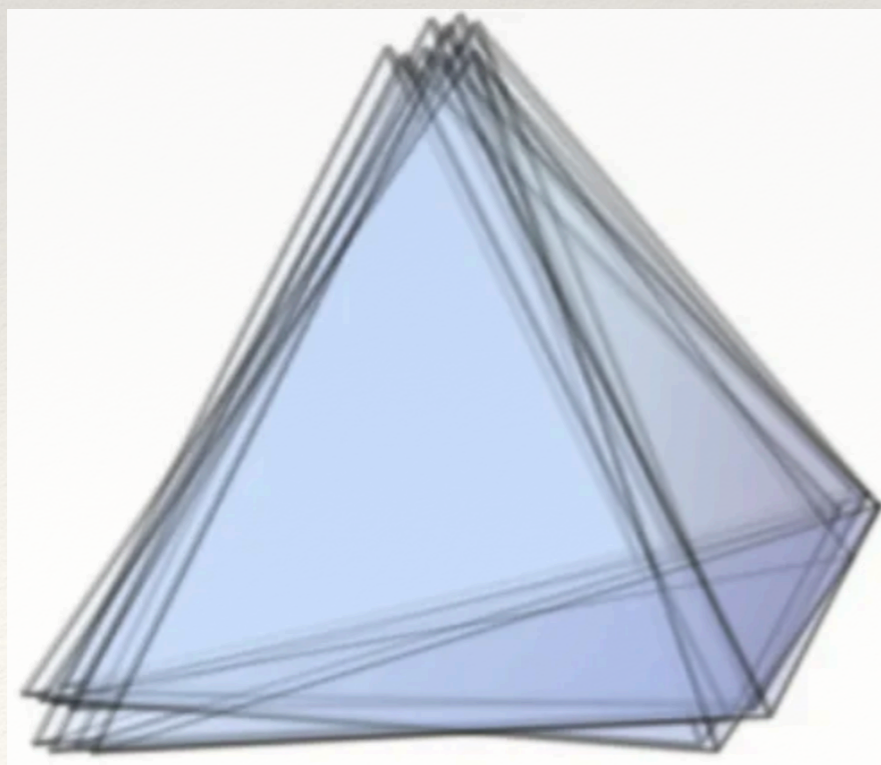
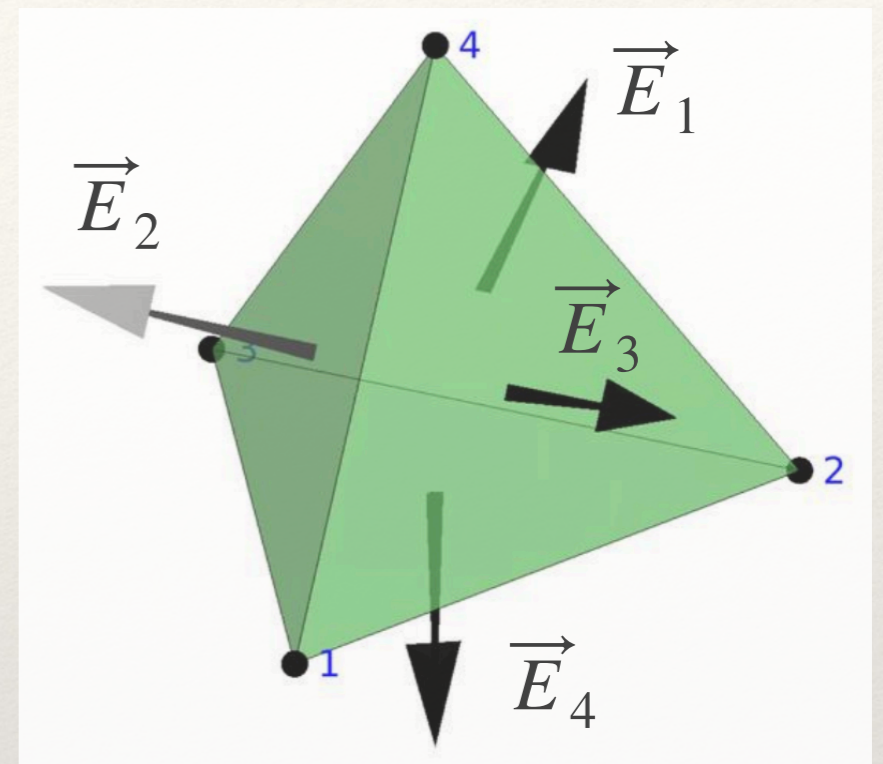
Review question 2: Where was the cat hiding in quantum gravity?

A tet satisfies closure:

$$\vec{E}_1 + \vec{E}_2 + \vec{E}_3 + \vec{E}_4 = 0.$$

Quantize a la SU(2) angular mom.:

$$|\hat{\mathbf{E}}_\ell| |j_\ell m_\ell\rangle = \gamma a_P \sqrt{j_\ell(j_\ell + 1)} |j_\ell m_\ell\rangle$$



New ingredient *intertwiners*:

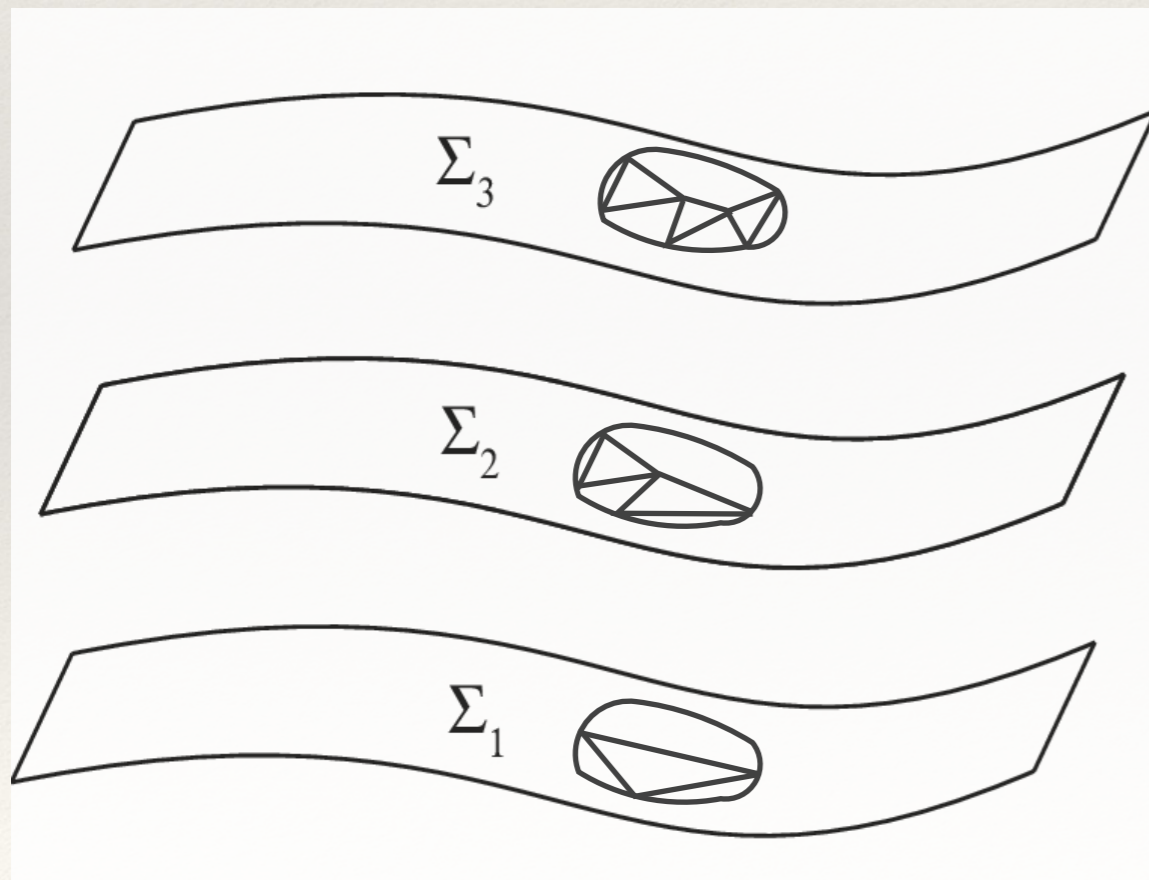
$$|i\rangle \in \text{Inv}(\mathcal{H}_{j_1} \otimes \mathcal{H}_{j_2} \otimes \mathcal{H}_{j_3} \otimes \mathcal{H}_{j_4})$$

E.g. the volume of the tet v ,

$$|i\rangle = |v j_1 j_2 j_3 j_4\rangle.$$

Summary Point: What are the observables we will work with?

Integrals of the A_a^i connection along loops are gauge invariant, and diffeomorphically inequivalent loops are the only distinct classes, thus, these make up a reasonable set of observables.



Spin networks provide a basis of indep loops. They carry $SU(2)$ irrep labels that give the area flux through surfaces transverse to the edges and intertwiners at the nodes that give the quantum numbers of the node, e.g. volume.

Prologue

Today I want to discuss the geometry of spacetime and dynamics. We'll begin with a simplified example...

Einstein dynamics—In a local inertial frame the Einstein equations can be given a particularly simple form:

$$\left. \frac{\ddot{V}}{V} \right|_{t=0} = -\frac{1}{2} (\rho + P_x + P_y + P_z),$$

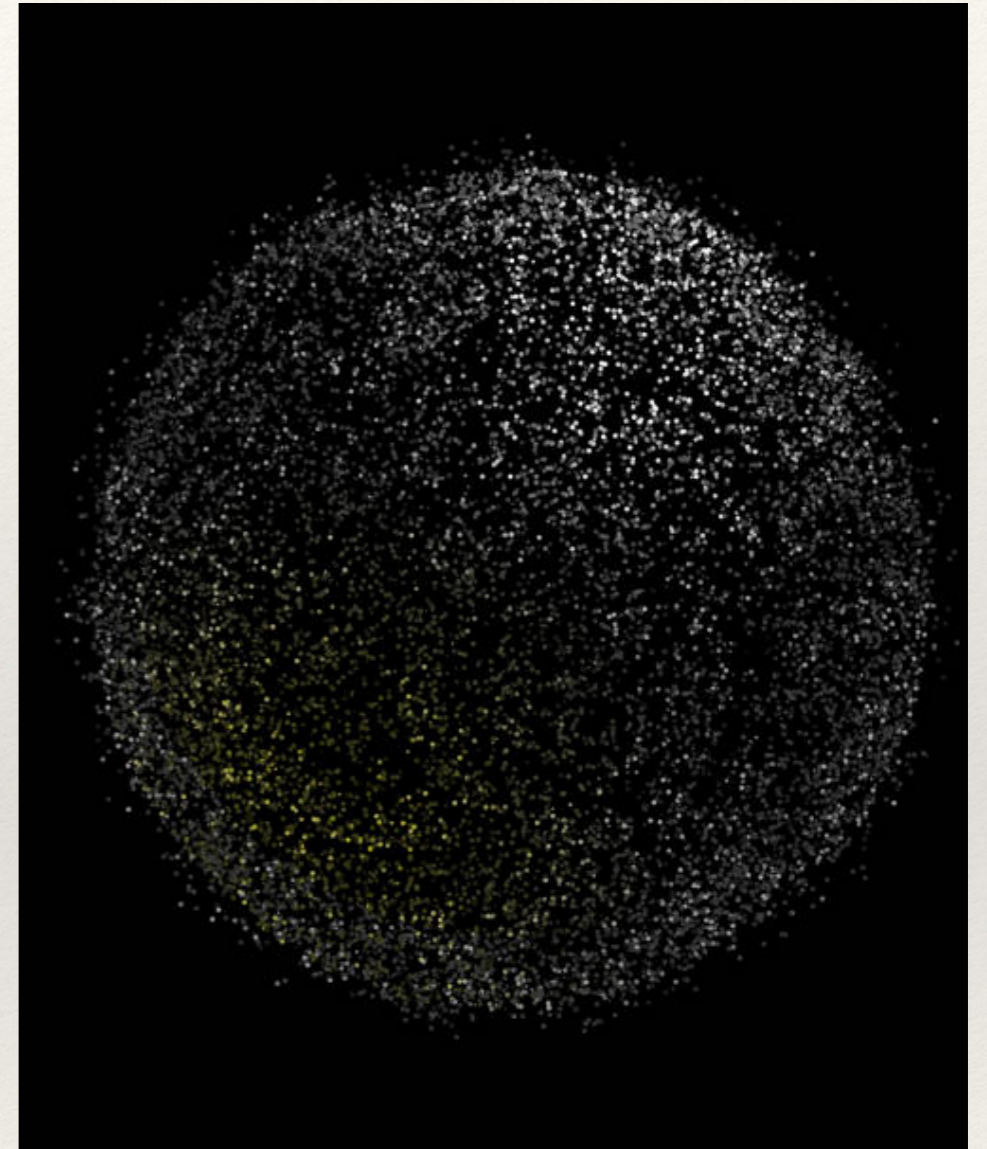
[Baez & Bunn AJP, 73 644]

where $V(t)$ is the spatial volume of a ball of test particles initially at rest, evolving with respect to the proper time of the central particle, and ρ & P_i are the energy density & pressures in the region.

In the absence of stress-energy

$$\ddot{V}|_{t=0} = 0$$

and the volume of the ball is constant to 2nd order in time. For example, a passing gravitational wave deforms the ball into an ellipsoid, preserving its volume.



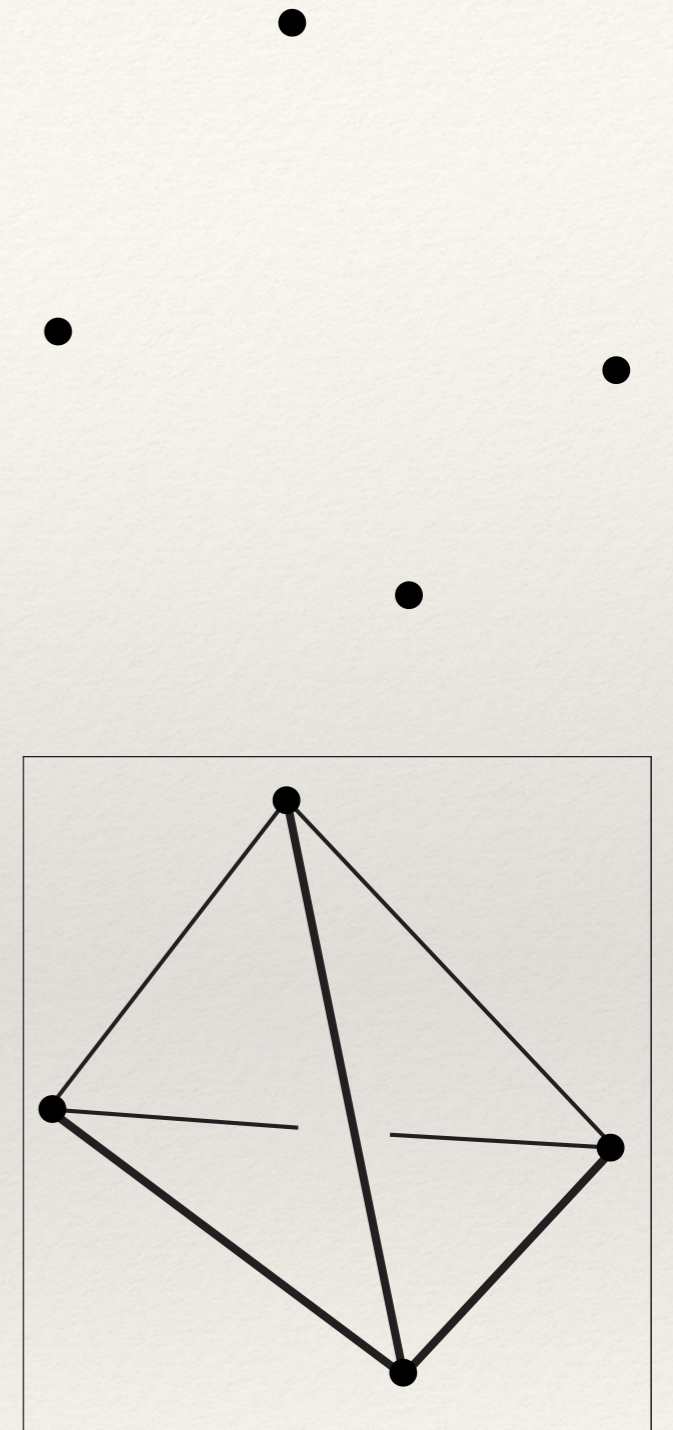
Truncating degrees of freedom

Now imagine removing most of the test particles, leaving just 4 behind.

If you only observe these 4 test particles, you will not have a window on all of the degrees of freedom of the gravitational field—just the ones that these particles betray.

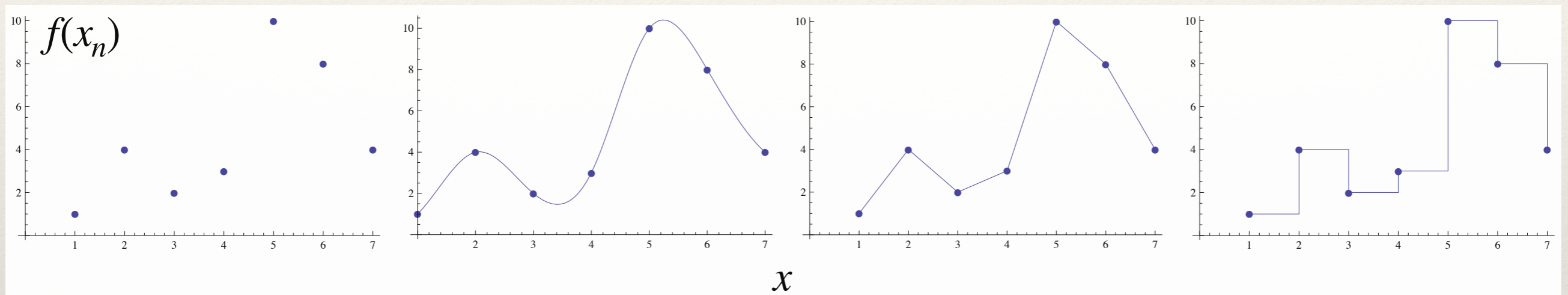
A *choice* that you can make is to interpolate these 4 particles with a tet.

But, it is essential to keep in mind that this is a choice.



An example helps to illustrate the point

In signal processing, you frequently interpolate a discrete signal with different convenient choices of continuous signal:



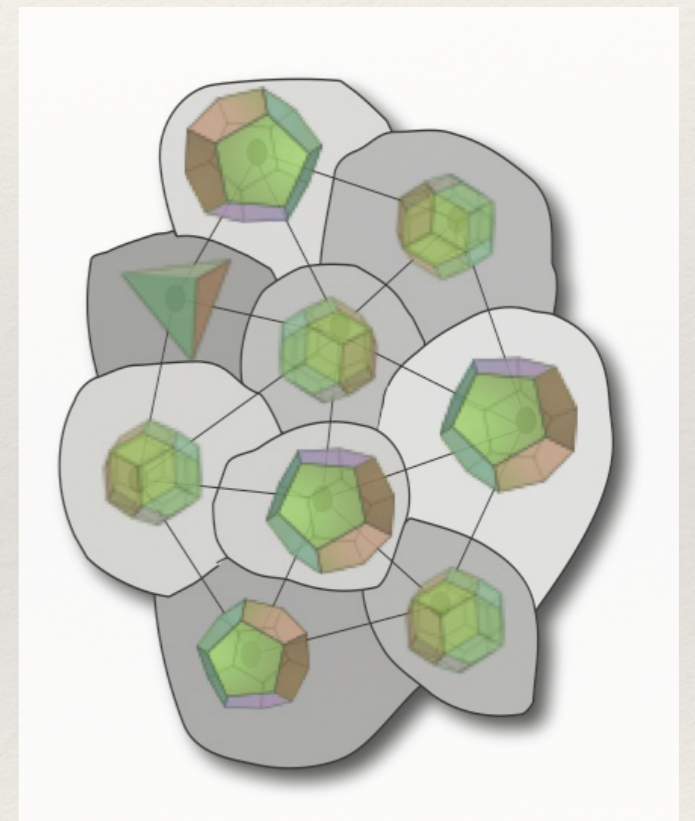
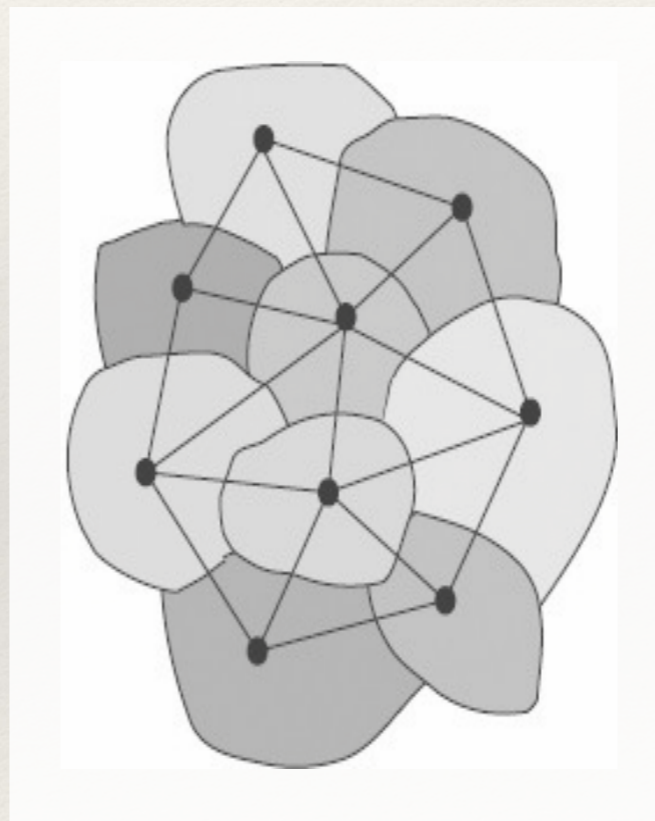
[Rovelli & Speziale, PRD 82]

We frequently do this in physics too. The various interpolations are: polynomial, like the mode expansion in cosmology; piecewise linear, like Regge calculus in GR; and piecewise flat, like twisted geometries in LQG.

So, there are different types of **discreteness** in **loop gravity** that richly interplay

When we work on a fixed graph Γ , we are truncating the infinite degrees of freedom of the classical gravitational field down to a finite number.

Polyhedra are just one choice for describing the captured geometrical degrees of freedom. Others are available.



Loop gravity also predicts an **observable discreteness**: the quantum, spectral discreteness of $|\hat{\mathbf{E}}_\ell|$ and of \hat{V} .

Today's Discussion

1. Building Space Part II: Spin Networks
2. The Tetrahedral Anomaly
3. Discrete Geometry Path Integrals: Spin Foams

Today's Discussion

1. Building Space Part II: Spin Networks

2. The Tetrahedral Anomaly

3. Discrete Geometry Path Integrals: Spin Foams

Much of loop gravity is constructed in parallel with **lattice gauge theory (LGT)**

Remarkable parallels with lattice gauge theory...:

1. Hilbert space is constructed over a graph Γ
2. Holonomies/Wilson loops (half) basic variables
3. Gauge invariance imposed at graph nodes

...but, also, key differences:

1. The quantum variables on the graph Γ give rise to spatial relations, not a consequence of them
2. **Importantly**, Γ is not endowed with a 'lattice spacing', no background metric structure

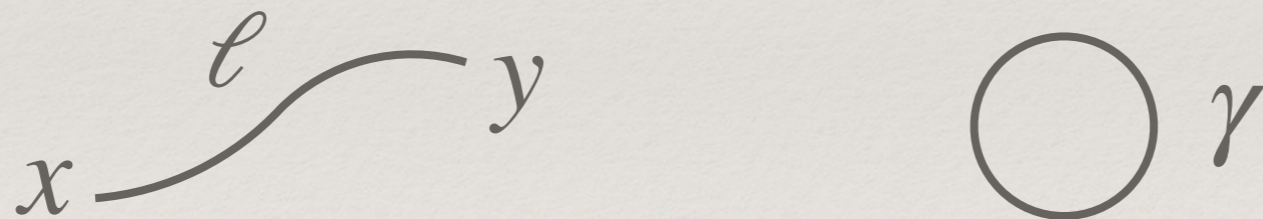
Similarities to lattice gauge theory: path ordering

We use Wilson loops as observables because of their invariance under gauge transformations:

$$A(x) \rightarrow g(x)A(x)g^{-1}(x) - g^{-1}(x)dg(x)$$

$$h_\ell(x, y) = \mathcal{P}e^{\int_x^y A} \rightarrow g(x)h_\ell(x, y)g^{-1}(y)$$

$$W(\gamma) = \text{tr} [g(x)h(x, x)g^{-1}(x)] = \text{tr} [h(x, x)]$$



The Ashtekar ‘ q ’ is an $SU(2)$ connection, hence non-abelian, and the holonomy h_ℓ will only have this nice transformation if we path order \mathcal{P} .

Similarities to lattice gauge theory: path ordering

Holonomies are group elements & should compose

$$x_1 \xrightarrow{\ell_1} x_2 \xrightarrow{\ell_2} x_3 \quad h_\ell = h_{\ell_1} h_{\ell_2}.$$

For an abelian connection this is immediate:

$$e^{A_1+A_2} = e^{A_1} e^{A_2}.$$

But, for a non-abelian connection, it's not so simple. You may have encountered the Baker-Campbell-Hausdorff result:

$$e^{A_1} e^{A_2} = e^{A_1+A_2+\frac{1}{2}[A_1,A_2]+\dots}.$$

Similarities to lattice gauge theory: path ordering

Path ordering restores $e^{A_1+A_2} = e^{A_1} e^{A_2}$ even in the non-abelian case. It is defined by

$$h(x, y) = \mathcal{P} e^{\int_x^y A} = \mathbb{1} + \int_0^1 ds A(s) + \int_0^1 ds_1 \int_{s_1}^1 ds_2 A(s_1) A(s_2) + \dots,$$

with $x \overset{\ell}{\curvearrowright} y$ parametrized by $s \in [0, 1]$.

Ex. 1 Take A constant along the path and show that the multiple integrals give $1/n!$ in this case.

Ex. 2 Take $A(s)$ to be A_1 if $s \in [0, 1/2)$ and A_2 if $s \in (1/2, 1]$ and show that you recover $e^{A_1+A_2} = e^{A_1} e^{A_2}$.

Similarities to lattice gauge theory

Working with holonomies h_ℓ there is a natural Hilbert space and inner product:

$$\mathcal{H} = L^2[G, \mu_H],$$

the space of square-integrable functions of the group elements with respect to the Haar measure μ_H .

We can extend this to a Hilbert space over a graph Γ with L links ℓ and N nodes n using the tensor product:

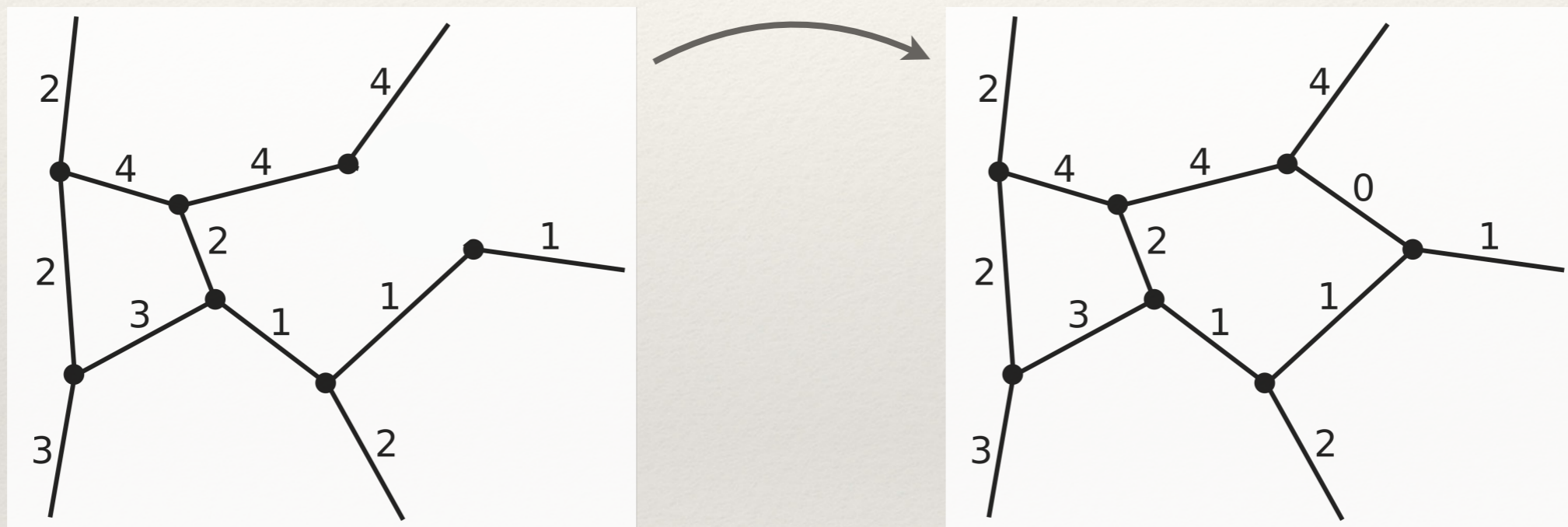
$$\mathcal{H}_\Gamma^L = L^2[G^L, \mu_H].$$

But, this space is not yet gauge invariant, so we finally divide by the gauge invariance at the nodes:

$$\mathcal{H}_\Gamma = L^2[G^L / G^N, \mu_H].$$

Similarities to lattice gauge theory

“Cylindrical consistency” allows us to extend this inner product to get notion of inner product on two different graphs Γ and Γ' . Idea:



Then,

$$\langle \Psi_{\Gamma}, \Psi_{\Gamma'} \rangle = \langle \Psi_{\Gamma}, \Psi_{\Gamma'} \rangle_{\Gamma''}.$$

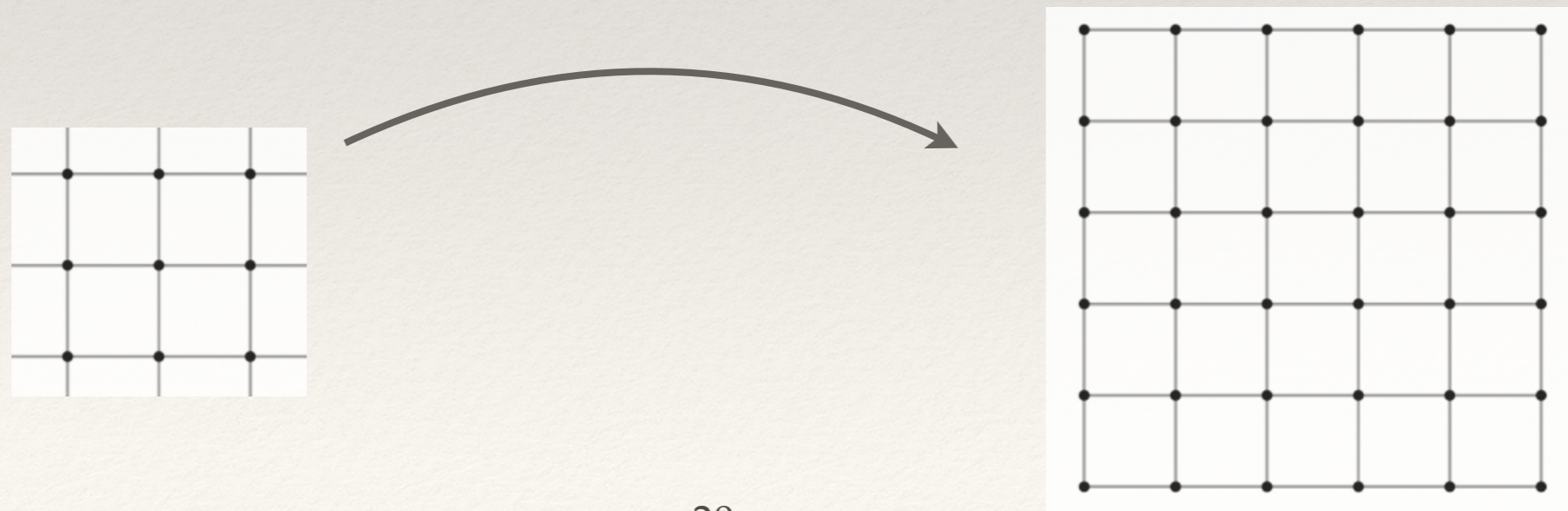
This allows a rich connection to continuum field theory in limit of finer and finer graph.

An important difference: in loop gravity there is no fixed lattice spacing

The lattice spacing l of LGT represents the metrical spacing of the points of the lattice.

There can be no such fixed background structure in a fully dynamical treatment of quantum gravity.

One consequence of this is that you refine the theory by increasing the number of nodes N of the graph, not changing the spacing l :



The key takeaway: well-defined construction of a kinematical Hilbert space

We have the Hilbert space:

$$\mathcal{H}_\Gamma = L^2[G^L/G^N, \mu_H],$$

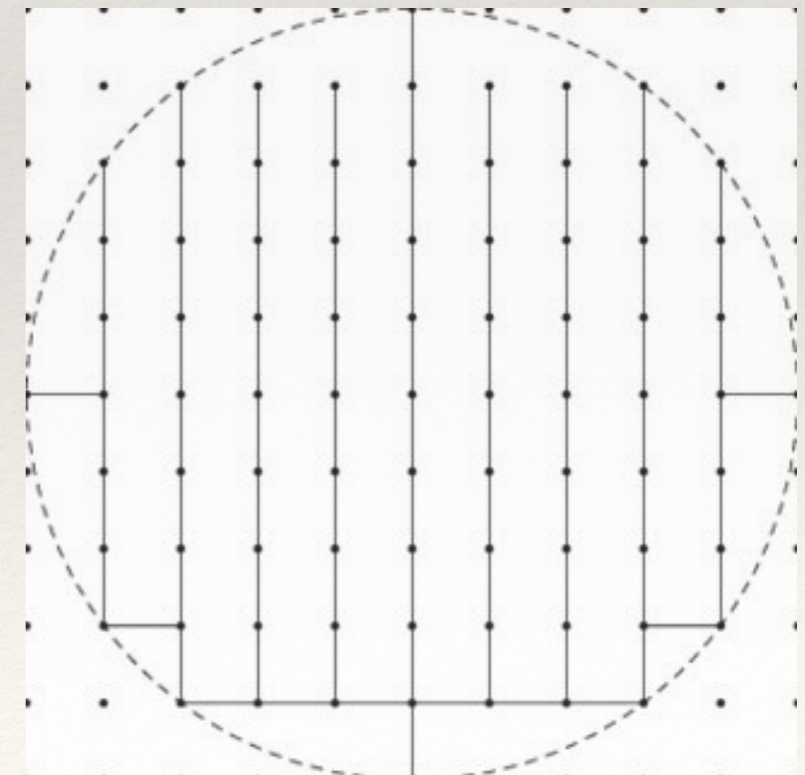
which consists of cylindrical functions:

$$f(A) = \Psi_\Gamma(\{h_\ell\}).$$

The holonomies probe the space time curvature around closed loops of the graph Γ

and

The fluxes probe the areas transverse to the links connecting nodes, which give 3D regions of space



Today's Discussion

1. Building Space Part II: Spin Networks

2. The Tetrahedral Anamoly

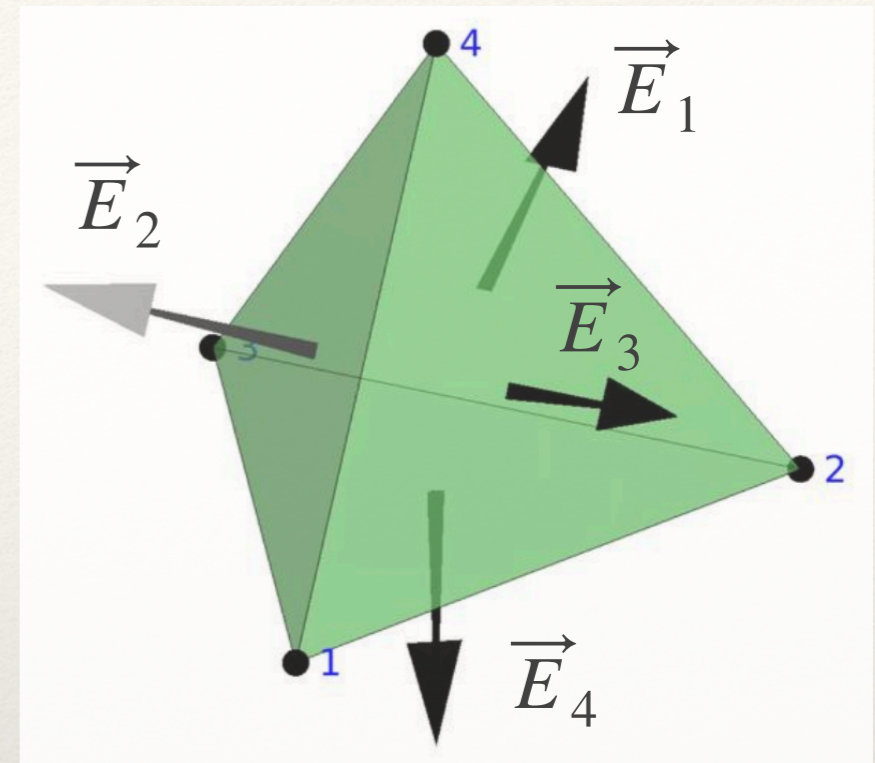
3. Discrete Geometry Path Integrals: Spin Foams

Warning: A change in notation

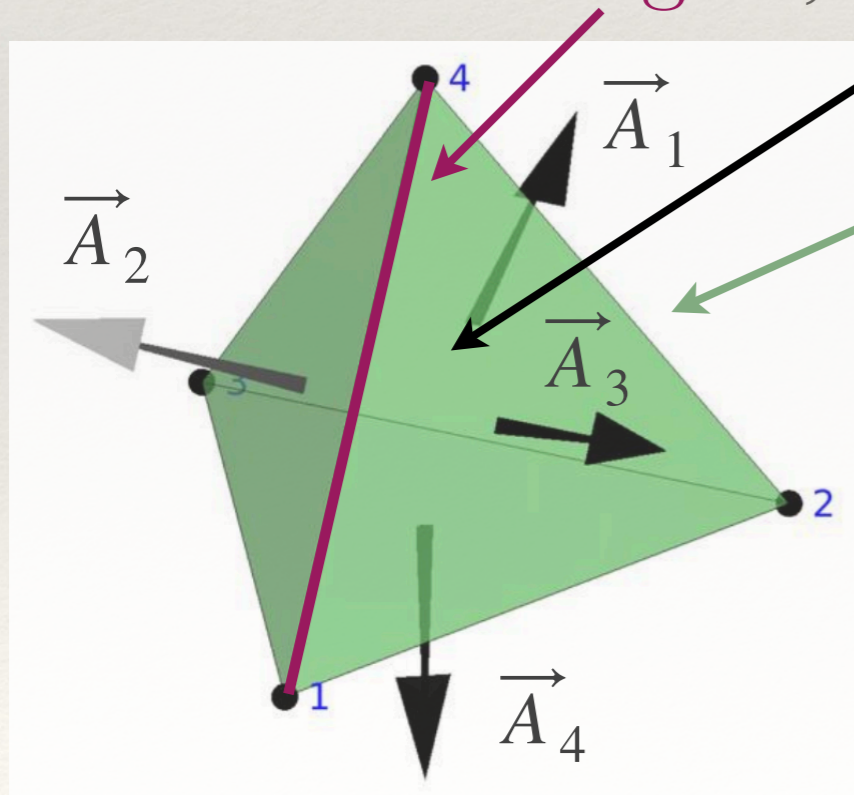
We have been studying the tetrahedron expressed in terms of electric fluxes:

$$\vec{E}_1 + \vec{E}_2 + \vec{E}_3 + \vec{E}_4 = 0.$$

Moving forward we will have less need to refer to the Ashtekar connection $A_a^i \dots$



more notation: edge e , triangle t , tet τ



...and so we will switch to a geometrical notation with:

$$\vec{A}_1 + \vec{A}_2 + \vec{A}_3 + \vec{A}_4 = 0.$$

This will make it more intuitive to refer to areas and ‘area vectors’.

The area vectors provide a unified framework for **Euclidean and Lorentzian** discrete geometries.

Taking $\vec{A}_t \in \mathfrak{so}(3)$ (Euclidean) or $\vec{A}_t \in \mathfrak{so}(2,1)$ (Lorentzian), the closure $\sum_t \vec{A}_t = 0$, expresses invariance in either case.

Counting the edge lengths, we know that a tetrahedron has 6 independent parameters. The 12 components $\{\vec{A}_t\}_{t=1}^4$ are clearly overkill, while the 4 magnitudes $\{A_t\}_{t=1}^4$ are insufficient.

Closure provides a way out of this quandary: there are precisely 6 independent vars

$$p_{tt'} = \text{sgn}(V_\tau^2) \vec{A}_t \cdot \vec{A}_{t'},$$

\swarrow $V_\tau = \text{the volume of tet } \tau$

due to the 4 constraint equations $\vec{A}'_t \cdot \sum_t \vec{A}_t = 0$.

Closure provides a way out of this quandary: there are precisely 6 independent vars

$$p_{tt'} = \text{sgn}(V_\tau^2) \vec{A}_t \cdot \vec{A}_{t'},$$

due to the 4 constraint equations $\vec{A}_{t'} \cdot \sum_t \vec{A}_t = 0$.

Count: $16 p_{tt'} - 6$ (symmetry) $- 4$ (relations) $= 6$ vars.

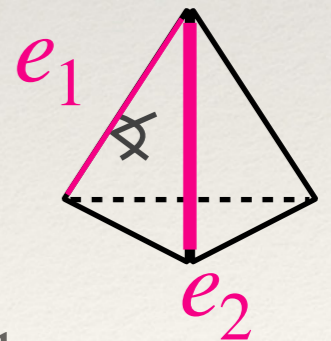
Four of these variables are the diagonal $p_{tt} = A_t^2$, i.e. 4 areas; the other 2 can be taken to be p_{e_1} and p_{e_2} with

$$p_e \equiv p_{tt'} = \text{sgn}(V_\tau^2) \vec{A}_t \cdot \vec{A}_{t'}, \quad e = t \cap t'$$

and $\{e_1, e_2\}$ a pair of *non*-opposite edges in τ .

The p_e are more convenient than the, perhaps,

more familiar 3D dihedral angles $\phi_e = \cosh^{-1}/\cos^{-1}(p_e)$.

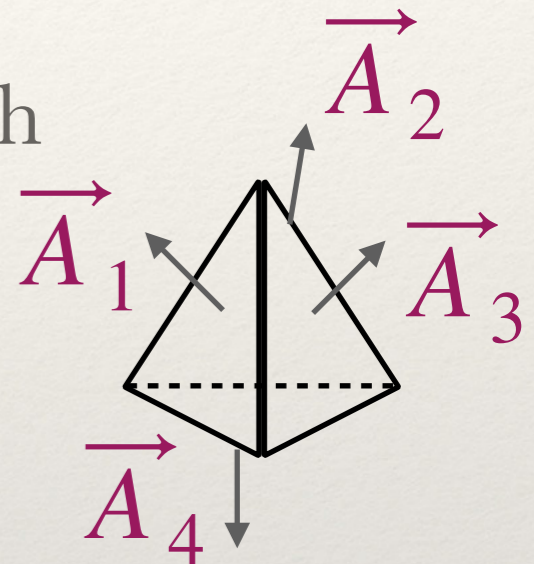


Intriguingly, the quantum area geometry of tetrahedra is **non-commutative**. We can see this by looking into the variables p_e .

As we just saw the areas A_t and 2 inner products p_{e_1}, p_{e_2} completely describe a tetrahedron τ : $p_{tt'}^\tau \equiv p_e^\tau = \text{sgn}(\text{Vol}_\tau^2) \hat{n}_t \cdot \hat{n}_{t'}$, & $p_{tt}^\tau = A_t^2$.

The area vectors satisfy $\{A_t^i, A_t^j\} = \gamma c_k^{ij} A_t^k = \gamma \epsilon^{ijm} \kappa_{mk} A_t^k$ with

$$\kappa_{ij} = \begin{cases} \delta_{ij} & \text{if Euclidean} \\ \eta_{ij} & \text{if Lorentzian} \end{cases}$$

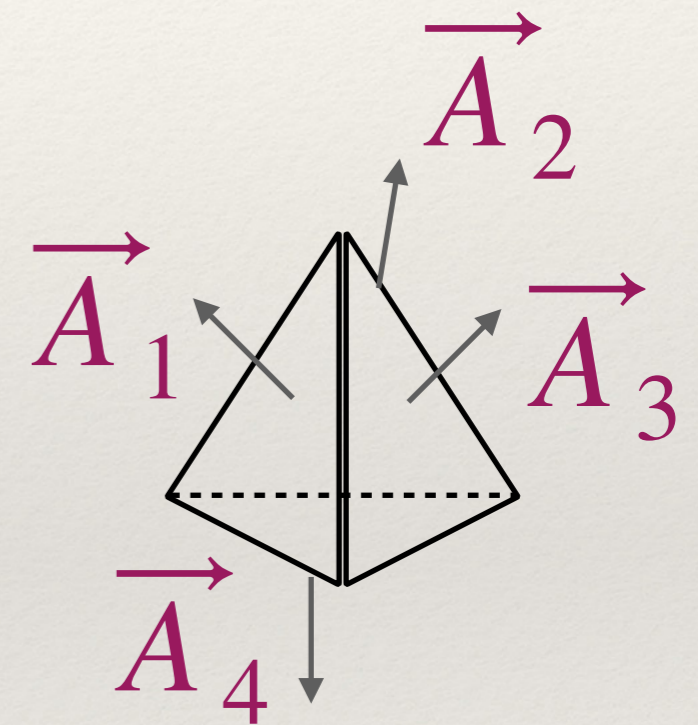


For a triple of triangles (t, t', t'') with angle parameters $p_{tt'}^\tau$ and $p_{t't''}^\tau$:

$$\begin{aligned} \{p_{tt'}^\tau, p_{t't''}^\tau\} &= \kappa_{ii'} \kappa_{jj'} A_{t'}^i A_{t''}^j \{A_t^{i'}, A_t^{j'}\} = \gamma \epsilon^{i'j'k'} \kappa_{ii'} \kappa_{jj'} \kappa_{kk'} A_{t'}^i A_{t''}^j A_t^k \\ &= \gamma \vec{A}_t \cdot (\vec{A}_{t'} \times \vec{A}_{t''}) = \pm \gamma \frac{9}{2} \text{Vol}_\tau^2 \end{aligned}$$

For fixed areas these degrees of freedom *do not commute*. Quantum mechanically they encode the shape of a fuzzy quantum tetrahedron.

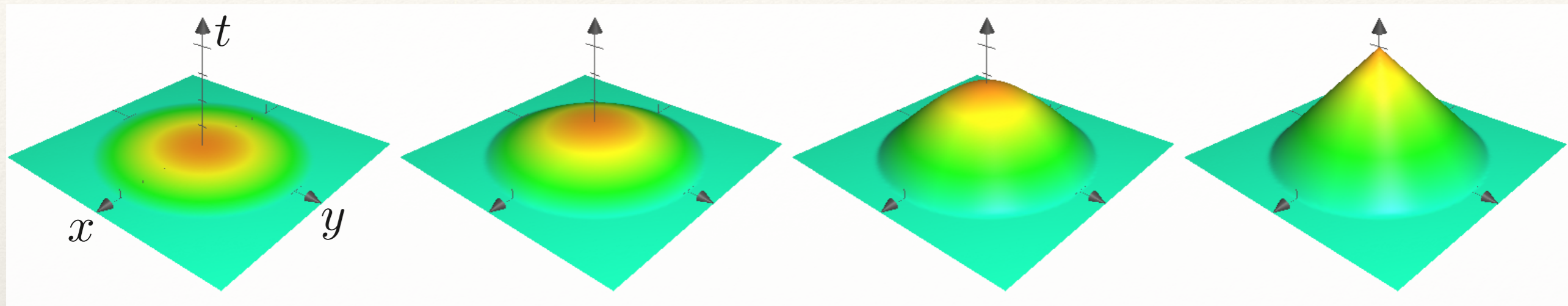
We will soon see that this means that the tetrahedral ‘cat’ leaves its paw prints everywhere...



Today's Discussion

1. Building Space Part II: Spin Networks
2. The Tetrahedral Anomaly
3. Discrete Geometry Path Integrals: Spin Foams

The prospect of a geometrical path integral is a constant source of ideas and challenges in quantum gravity



Fixing a region of spacetime and some aspects of the geometry on its boundary (e.g. the boundary metric), we aim to sum over all spacetime geometries that interpolate these boundary data:

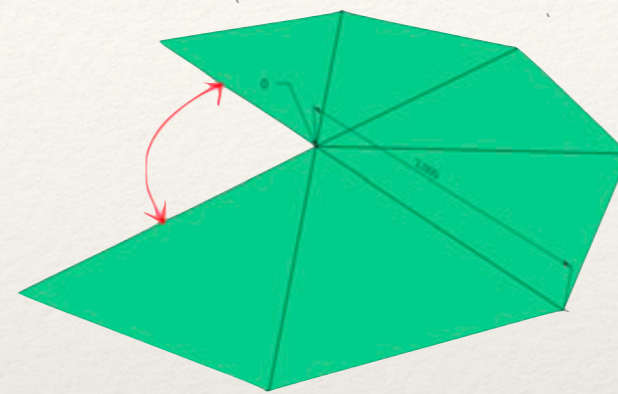
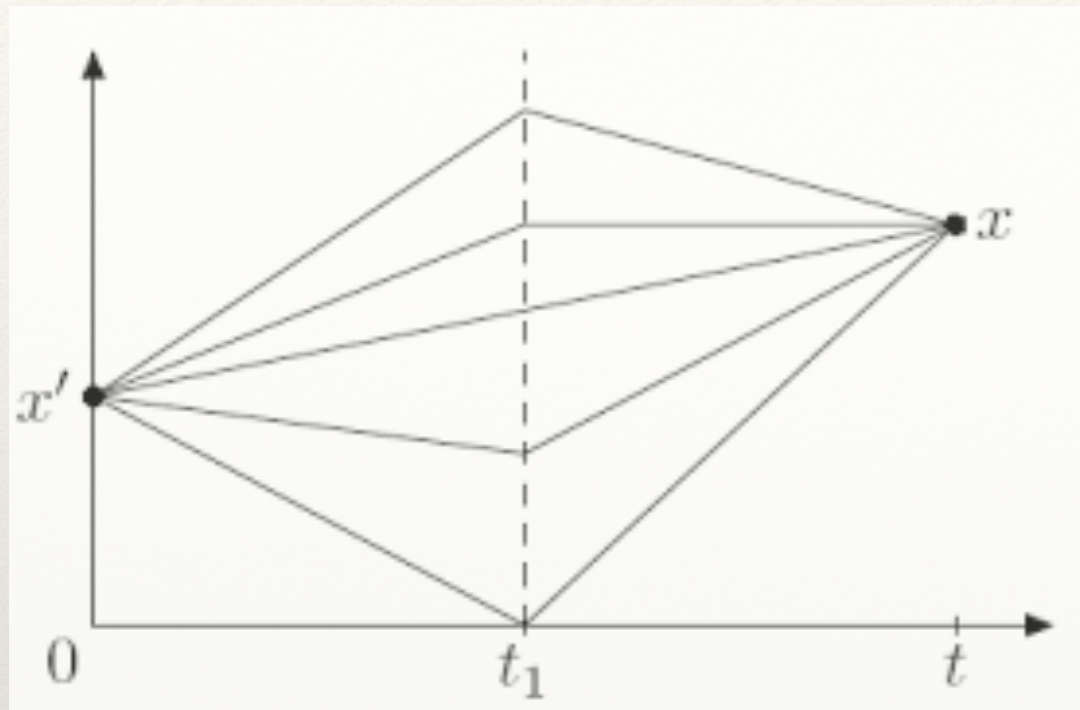
$$\mathcal{Z} = \int \mathcal{D}\text{geom} \exp \{ iS(\text{geom}) \}.$$

What is the most convenient set of variables to work with?

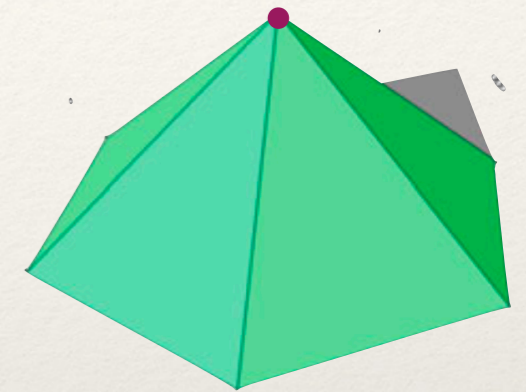
How should we describe the space of (unique) geometries?

How do we properly compose regions to build up larger regions?

A compelling principle providing the answer to all of these questions at once still seems to be missing...



2D



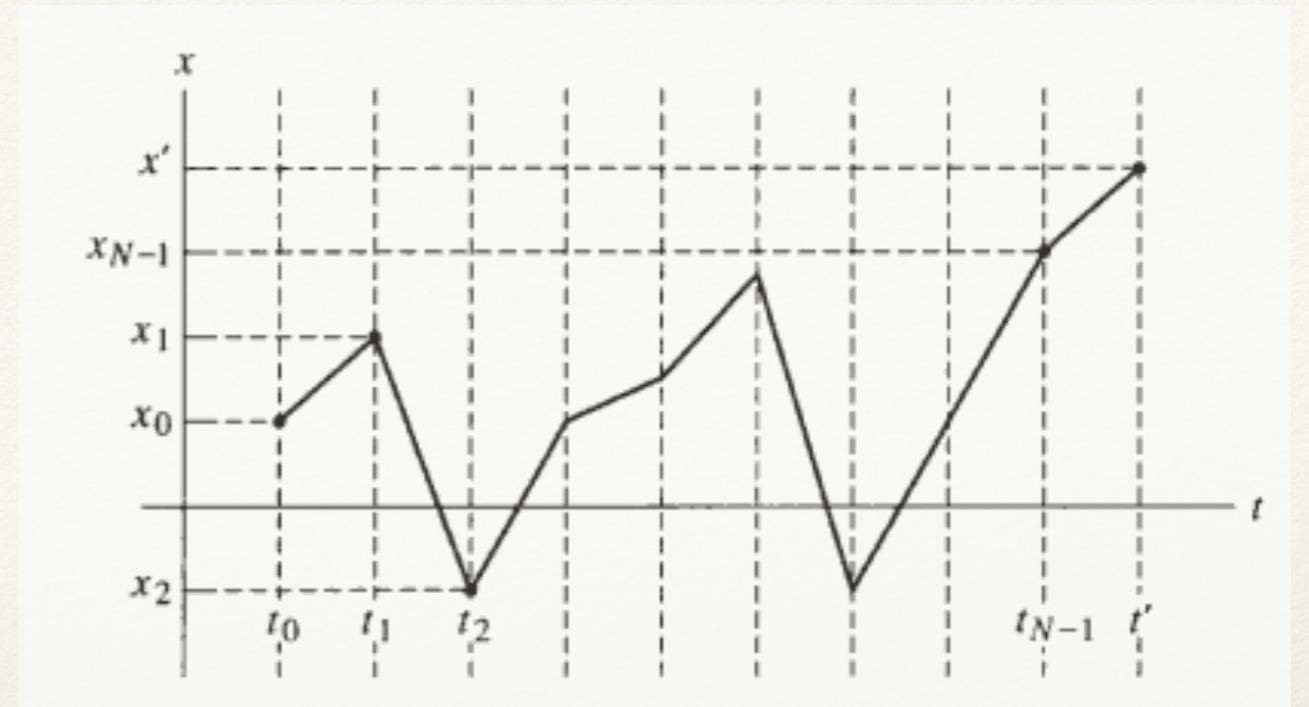
...however, we can take inspiration from Feynman's slit screen idea and its simplification of classical trajectories.

Instead of considering everywhere curved surfaces, we imagine building up curvature out of flat pieces. This idea has a long history, but there is still much to learn of the choices involved.

The additive factorization of the action,

$$\sum_{k=1}^N \left[\frac{m}{2} \left(\frac{x_k - x_{k-1}}{\Delta t} \right)^2 - V(x_{k-1}) \right],$$

greatly aids in carrying out a path integral:



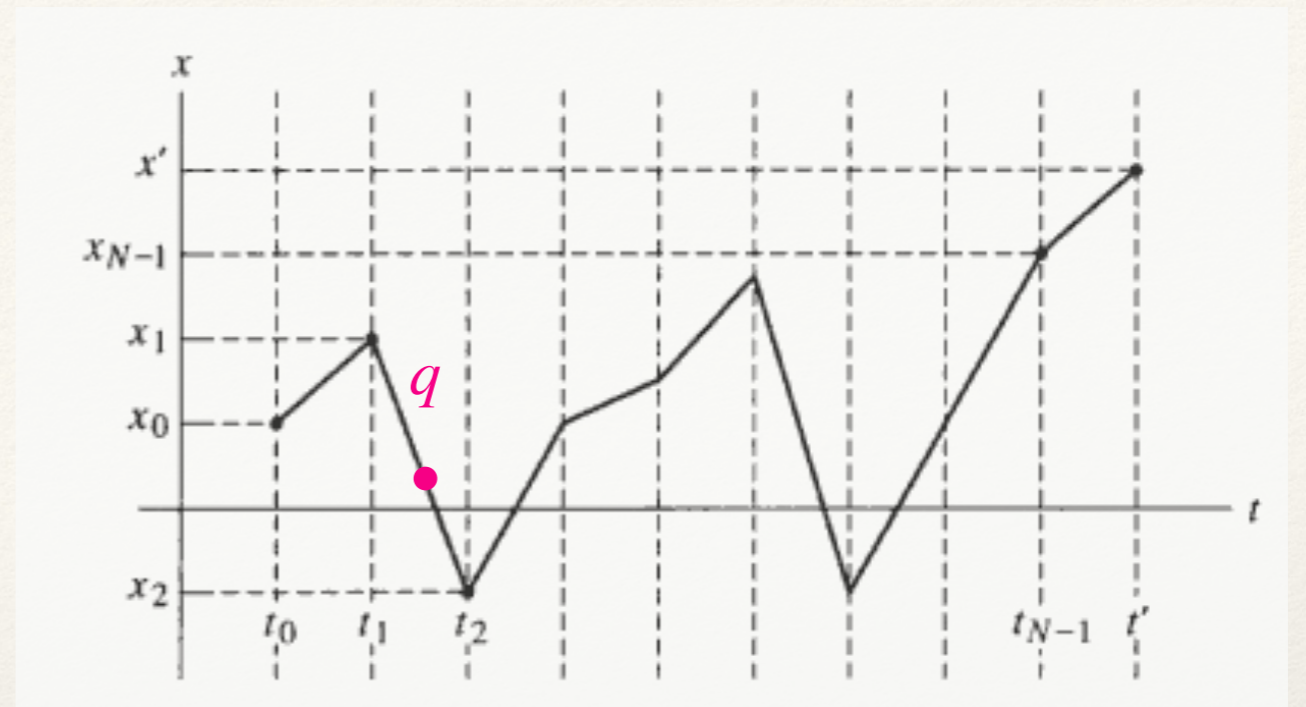
$$K(x', x, T) = \lim_{N \rightarrow \infty} \left(\frac{m}{i2\pi\hbar\Delta t} \right)^{\frac{N}{2}} \prod_{k=1}^{N-1} \int dx_k \exp \left(\frac{i}{\hbar} \Delta t \sum_{k=1}^N \left[\frac{m}{2} \left(\frac{x_k - x_{k-1}}{\Delta t} \right)^2 - V(x_{k-1}) \right] \right)$$

Indeed, were it not for the coupling of the intervals $(x_{k+1} - x_k)$ and $(x_k - x_{k-1})$ through x_k , we could factor this into a product of amplitudes for each interval.

Let us focus on one pair of these variables: x_1 and x_2 , say.

We can further decouple these variables by introducing an intermediate gluing point q

$$e^{-\frac{(x_2 - x_1)^2}{2(t_2 - t_1)}} = \frac{1}{\mathcal{N}} \int dq e^{-\frac{(x_2 - q)^2}{2t_2}} \cdot e^{-\frac{(q - x_1)^2}{2t_1}}$$



Several facets to q :

- ▲ From the perspective of the initial x variables, q further factorizes the x amplitudes; this, of course, at the cost of a new integration variable, the q .
- ▲ The discrete trajectory can bend further at q ; additional dynamics $V(q)$.
- ▲ A straight line trajectory is completely unaffected by introduction of q .
- ▲ The q variable can even be used to impose constraints on the segments it connects.

Geometrical Variables—Choosing variables in the geometrical path integral has myriad consequences

We will:

1. See how area variables lead to flat classical solutions in the unconstrained theory.
2. Study constraints on the classical theory cast in these variables and discover why they can only be imposed weakly in the quantum theory. This allows us to define a geometrical path integral.
3. Show that weak constraints lead to a surprisingly rich interplay of the model parameters in geometrical expectation values. Nonetheless, numerics show that classical geometries emerge in certain parameter regimes, evidence of good spin foam dynamics.
4. Present a newer spin foam model called an ‘effective spin foam’. This will be complementary to the many excellent introductions available in the literature to the EPRL-FK spin foam models.

[Perez, [Living Reviews in Relativity](#)]

In Regge Calculus we describe spacetime by a triangulation of flat pieces glued together to give curvature.

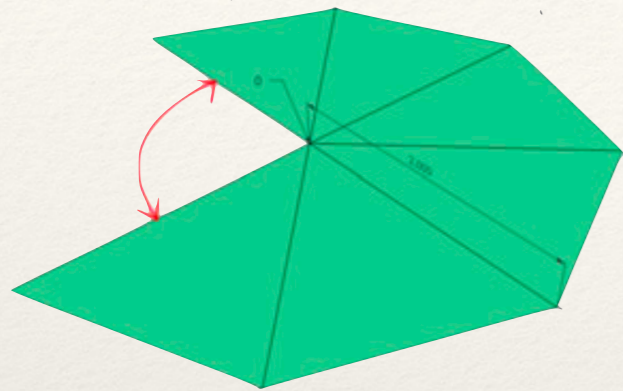
Regge Calculus

This, once again, cuts the degrees of freedom of gravity down to a finite number and greatly eases their study.

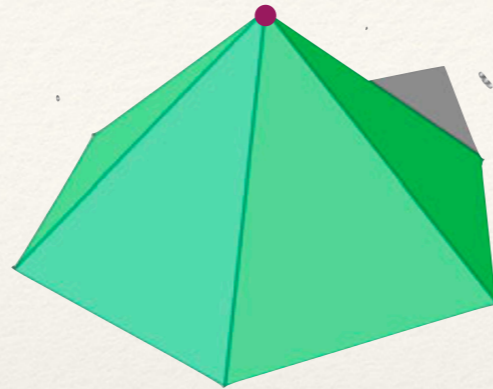
It is also essential for doing numerics.



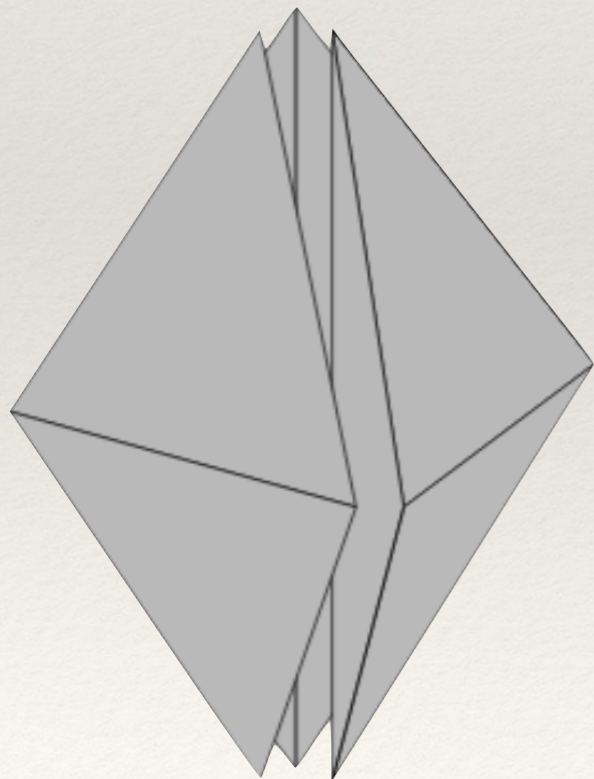
A dimensional ladder helps to illustrate some salient aspects of Regge Calculus



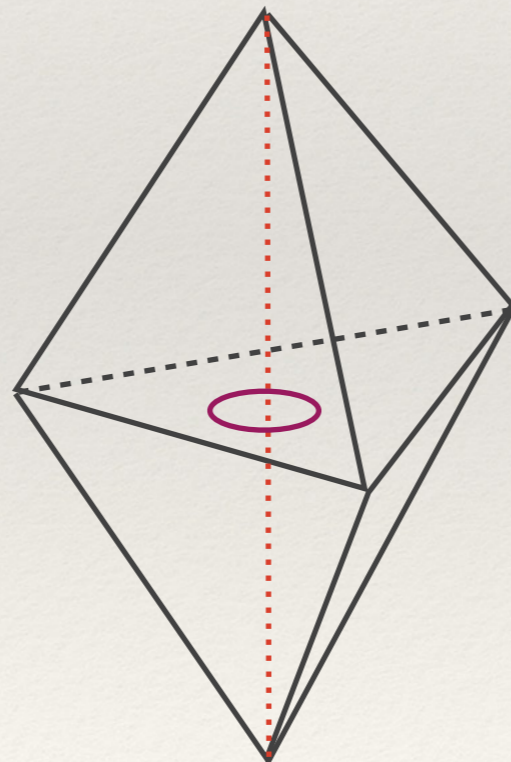
2D



In 2D it is clear how curvature becomes concentrated on the $(d - 2)$ -dimensional ‘bones’.



3D



In 3D we see an intriguing alignment between the *metrical* and *symplectic* aspects: the bones are 1D edges, whose lengths give the metric;

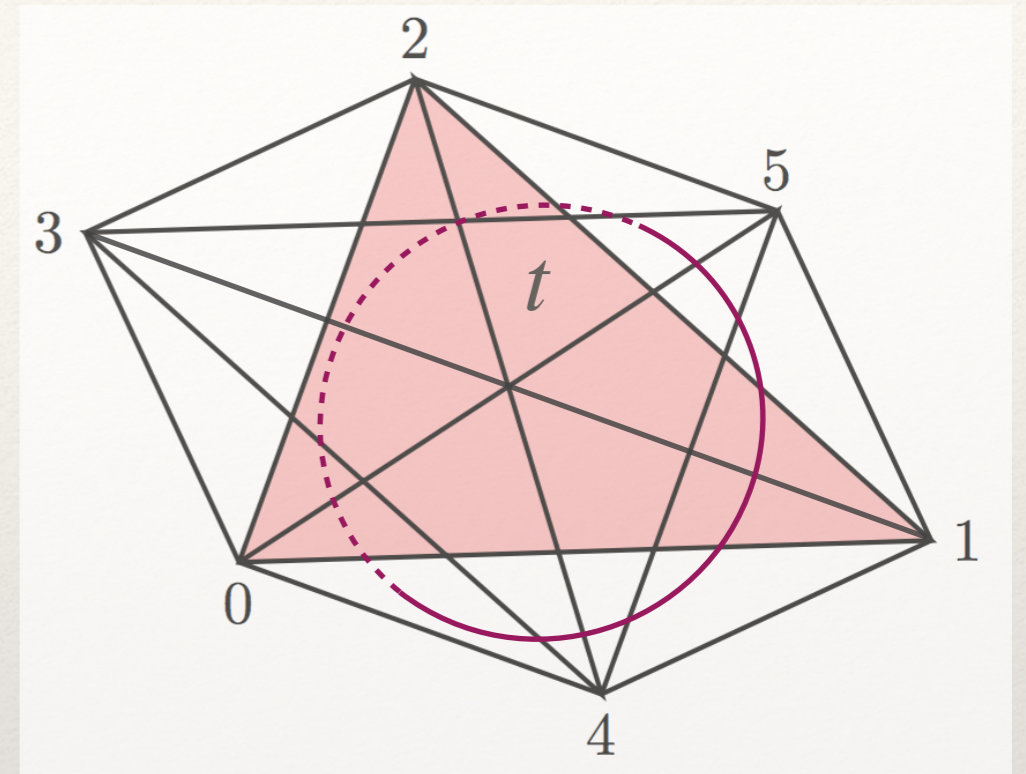
meanwhile the conjugate curvature angle is compact and leads to quantization of lengths

In 4D the bones are 2D triangles t .

One is forced to choose between:
the apparent metrical length
variables l , with a complicated
conjugate variable

or

The curvature angle around the
bone, which is conjugate to the
area of the triangle t . Again as the
curvature angle is compact, the
areas are quantized.



The 2nd choice is harmonious with LQG, and is the focus of
effective spin foam models.

In standard Regge Calculus we treat the lengths of edges as variables...

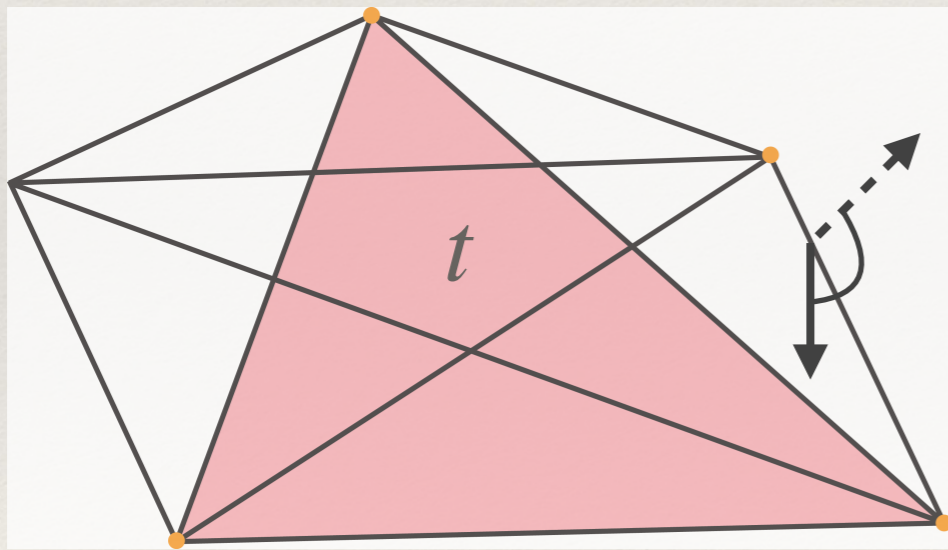
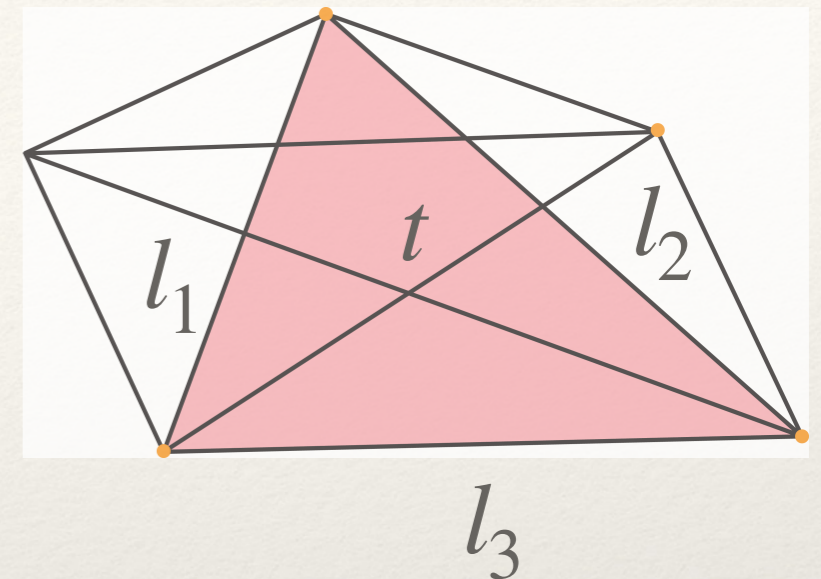
Area Regge Calculus

...in Area Regge Calculus it's the areas of triangles. This provides a closer connection to area geometry, its quantization, and loop quantum gravity.



In 4D we triangulate using 4-simplices—the 4D analog of tetrahedra—which are made up of 5 vertices, 10 edges, 10 triangles, and 5 tetrahedra.

Locally the functions $A_t(l)$ (c.f. Heron) can be inverted to give edge lengths $L_e^\sigma(a)$. Systems of such equations will, in general, give you a finite, discrete set of roots for the $L_e^\sigma(a)$.



The p_e (or 3D dihedral angles) of tetrahedra in the triangulation distinguish such roots, and we can consistently follow a root of interest.

[Recall Heron:

$$A_t^2(l_1, l_2, l_3) = \frac{1}{16}(l_1 + l_2 + l_3)(l_1 + l_2 - l_3)(l_1 - l_2 + l_3)(-l_1 + l_2 + l_3)]$$

The inversion of the last slide is what allows us to convert standard Length Regge Calculus into Area Regge Calculus

The Regge Action for a 4D triangulation Δ is

$$S_{\text{Regge}} = \sum_t A_t \epsilon_t,$$

where

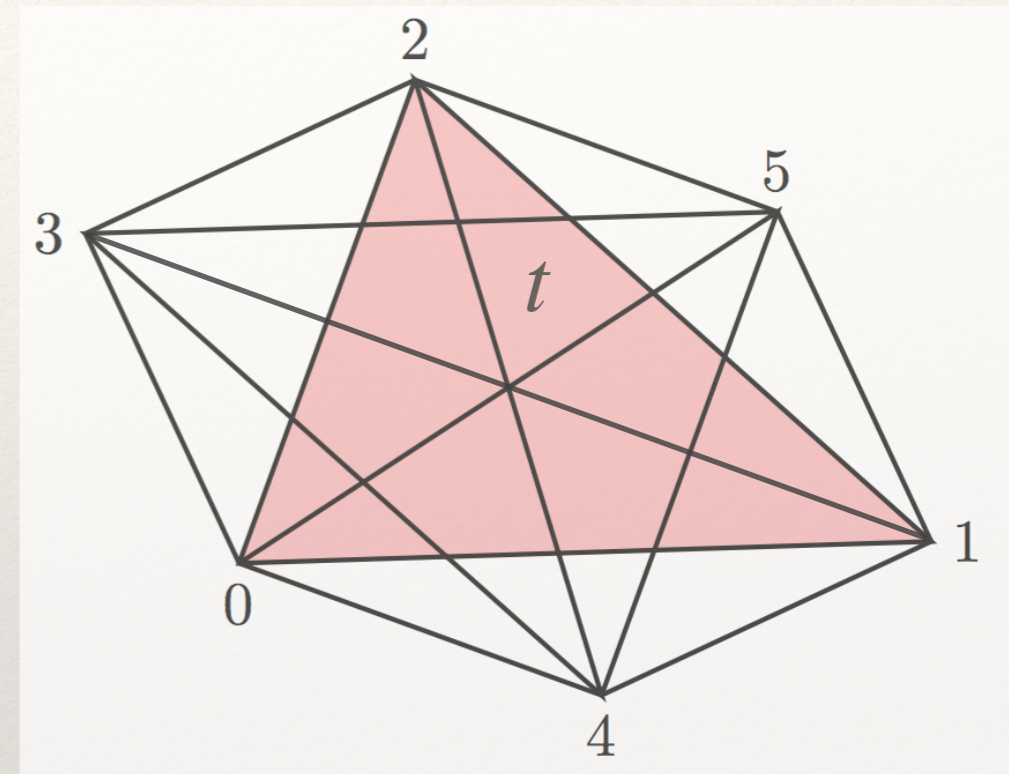
$$\epsilon_t = 2\pi - \sum_{\sigma \supset t} \theta_t^\sigma.$$

In Length Regge Calculus (LRC) we take

$$A_t = A_t(l) \quad \text{and} \quad \theta_t^\sigma = \theta_t^\sigma(l)$$

and varying S_{LRC} w.r.t. the bulk lengths l gives the eqs. of motion

$$\sum_{t \supset e} \frac{\partial A_t}{\partial l_e} \epsilon_t(l) = 0, \quad \text{which limit, for finer \& finer } \Delta, \text{ to the Einstein eqs.}$$



In standard Regge Calculus we treat the lengths of edges as vars, while in Area Regge Calculus it's the areas of triangles

A 4-simplex has ten edges and ten faces. Locally the functions $A_t(l)$ can be inverted to give edge lengths $L_e^\sigma(a)$.

Considering areas a as variables we can define Area Regge Calculus (ARC) via the action

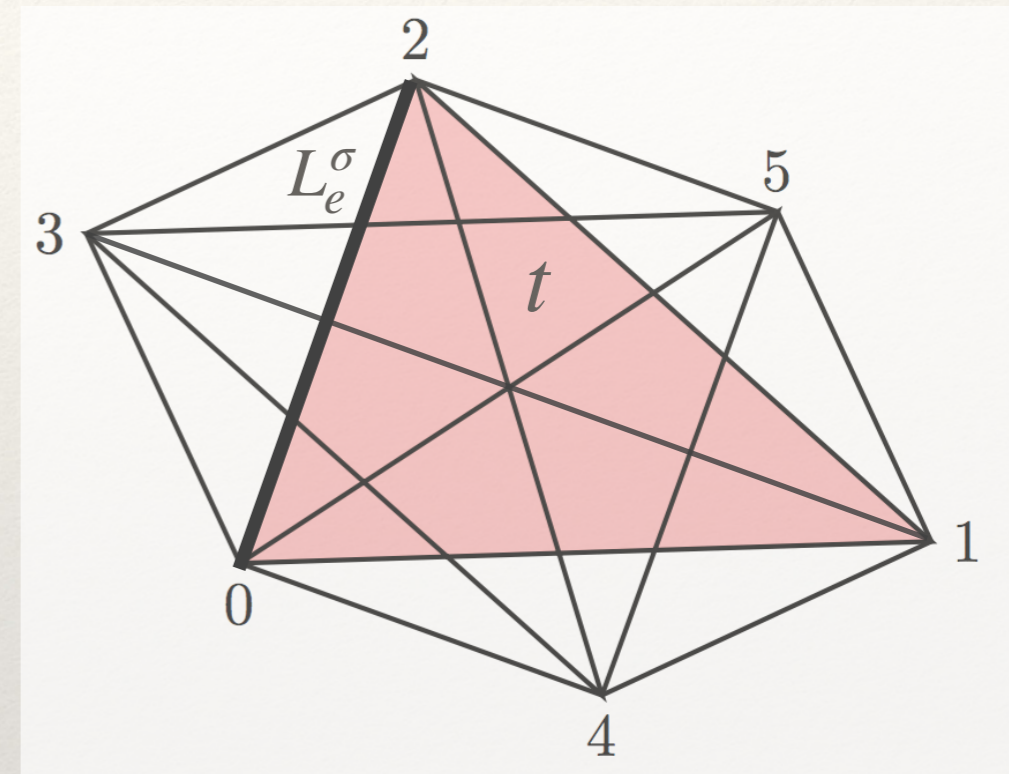
$$S_{\text{ARC}} = \sum_t a_t \epsilon_t(a) .$$

The dihedral and deficit angles are obtained using $\theta_t^\sigma(a) = \theta_t^\sigma(L^\sigma(a))$.

Strikingly, variation of this action gives eqs. of motion

$$\delta S_{\text{ARC}} = \epsilon_t(a) + \sum_t a_t \delta \epsilon_t = \epsilon_t(a) = 0, \quad \text{which impose flatness on } \Delta.$$

0 (due to the Schläfli identity)



Adding Constraints to the Theory

We can understand this difference in eqs. of motion between ARC and LRC as due to a differing # of degrees of freedom.

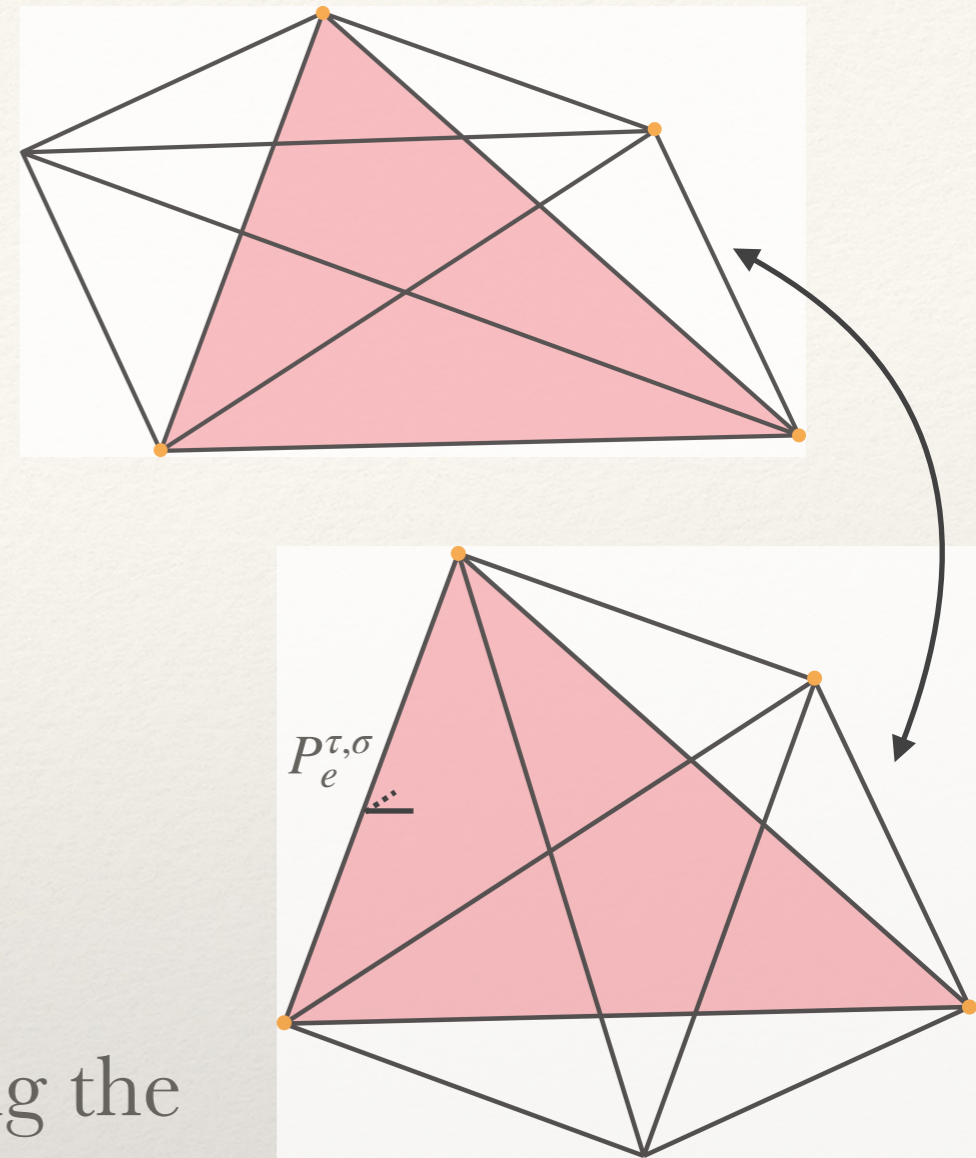
Gluing along the tetrahedron with orange vertices, 6 edge lengths are matched, but only 4 areas.

This mismatch can be resolved by introducing the dot products $p_{tt'}$:

$P_e^{\tau,\sigma}(a) = P_e^{\tau}(L^{\sigma}(a))$ is the dihedral angle around edge e in tet τ .

Two neighboring simplices $\{\sigma, \sigma'\}$, glued along τ , will have the same lengths in τ if the constraints

$$P_{e_i}^{\tau,\sigma}(a) - P_{e_i}^{\tau,\sigma'}(a) = 0, \quad i = 1, 2 \text{ are imposed on non-opposite edges } e_i.$$



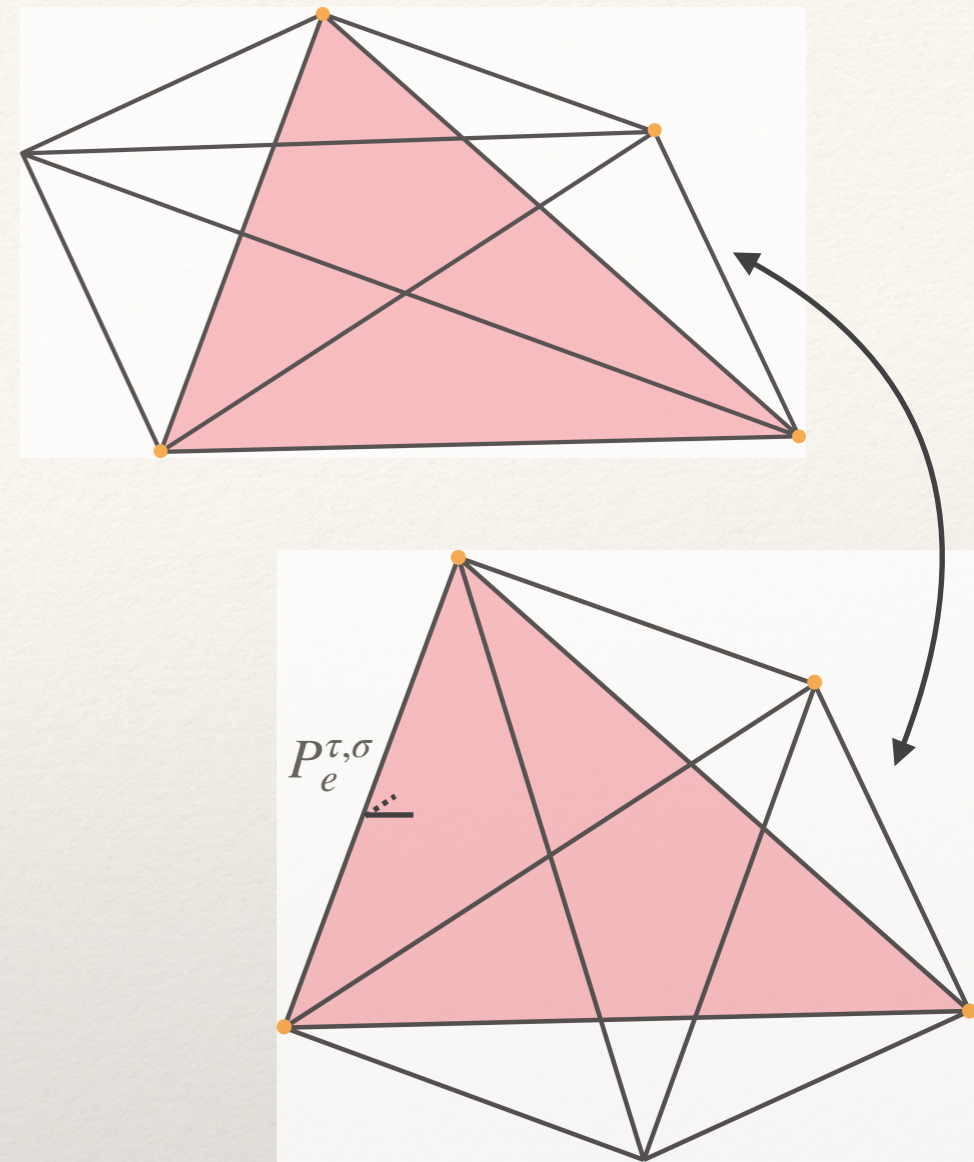
ARC with these constraints imposed leads to the same equations of motion as LRC.

But, imposing

$$P_{e_i}^{\tau,\sigma}(a) - P_{e_i}^{\tau,\sigma'}(a) = 0, \quad i = 1,2$$

at non-opposite edges e_i leads to highly non-local constraints on the theory with the geometry of tetrahedron τ being fixed by area variables throughout the simplices σ and σ' . We don't want this.

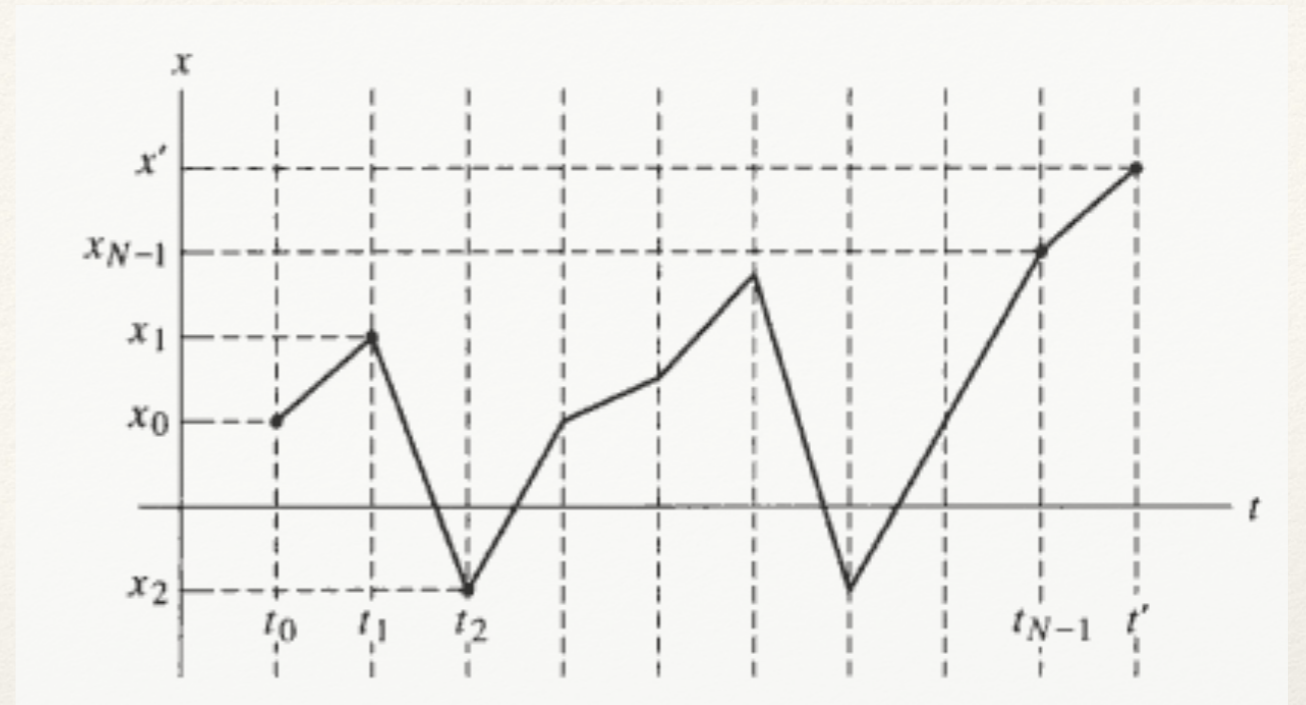
Returning to our comparison with the path integral in 1D Quantum Mechanics is useful here...



The additive factorization of the action,

$$\sum_{k=1}^N \left[\frac{m}{2} \left(\frac{x_k - x_{k-1}}{\Delta t} \right)^2 - V(x_{k-1}) \right],$$

greatly aids in carrying out a path integral:



$$K(x', x, T) = \lim_{N \rightarrow \infty} \left(\frac{m}{i2\pi\hbar\Delta t} \right)^{\frac{N}{2}} \prod_{k=1}^{N-1} \int dx_k \exp \left(\frac{i}{\hbar} \Delta t \sum_{k=1}^N \left[\frac{m}{2} \left(\frac{x_k - x_{k-1}}{\Delta t} \right)^2 - V(x_{k-1}) \right] \right)$$

We noticed that were it not for the coupling of the intervals $(x_{k+1} - x_k)$ and $(x_k - x_{k-1})$ through x_k , we could factor this into a product of amplitudes for each interval.

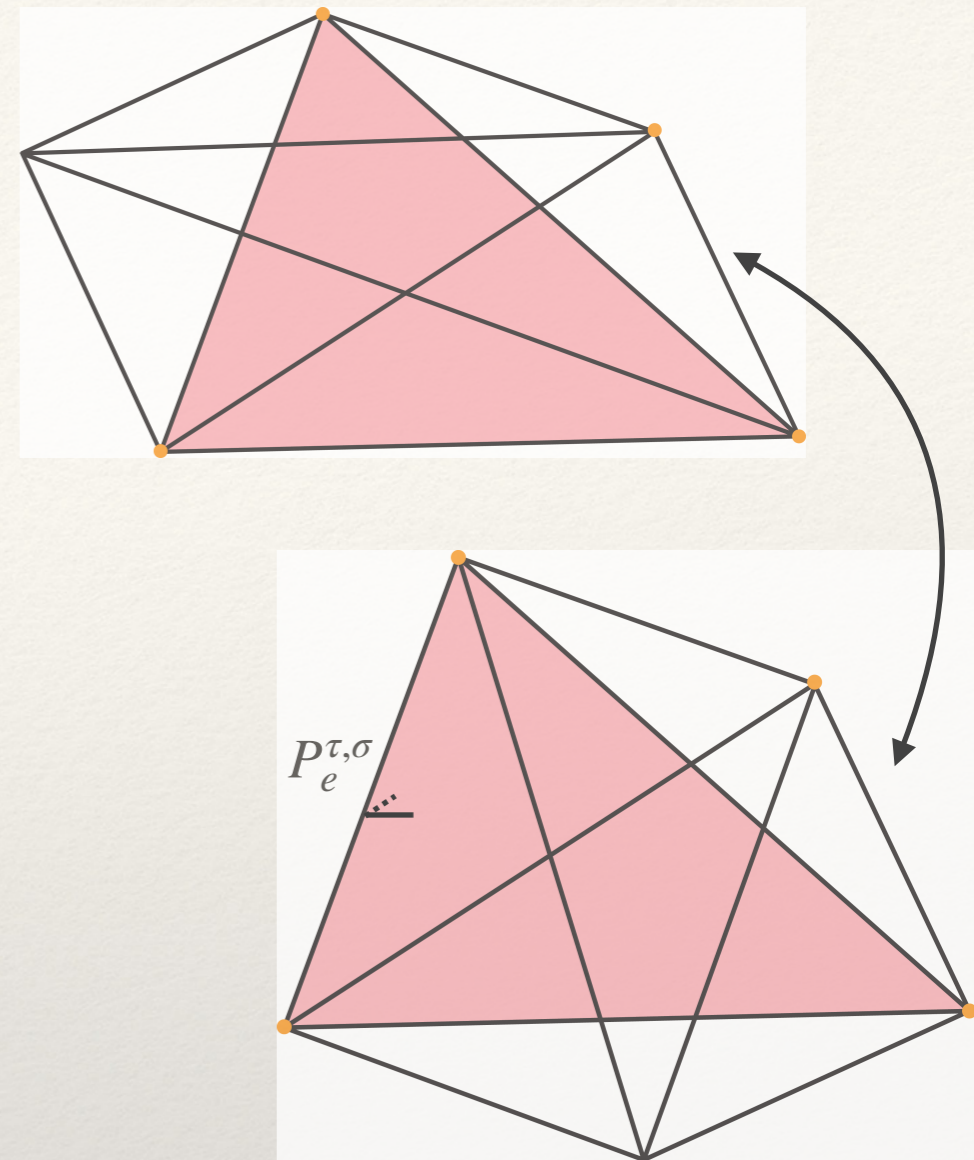
We can localize constraints to a single 4-simplex by introducing the two additional variables $p_{e_i}^\tau$ per τ to our theory and imposing

$$\mathcal{C}_i \equiv p_{e_i}^\tau - P_{e_i}^{\tau,\sigma}(a) = 0, \quad i = 1, 2.$$

The advantage of these localized constraints is that they preserve additive factorization of the Regge action and allow us to write the path integral in a product factorized form.

Importantly, as we've seen, dot products at a pair of non-opposite edges (e_1, e_2) do not commute. Instead

$$\{p_{e_1}^\tau, p_{e_2}^\tau\} = \pm \gamma \frac{9}{2} \text{Vol}_\tau^2, \quad \text{with } (e_1, e_2) \text{ non-opposite.}$$



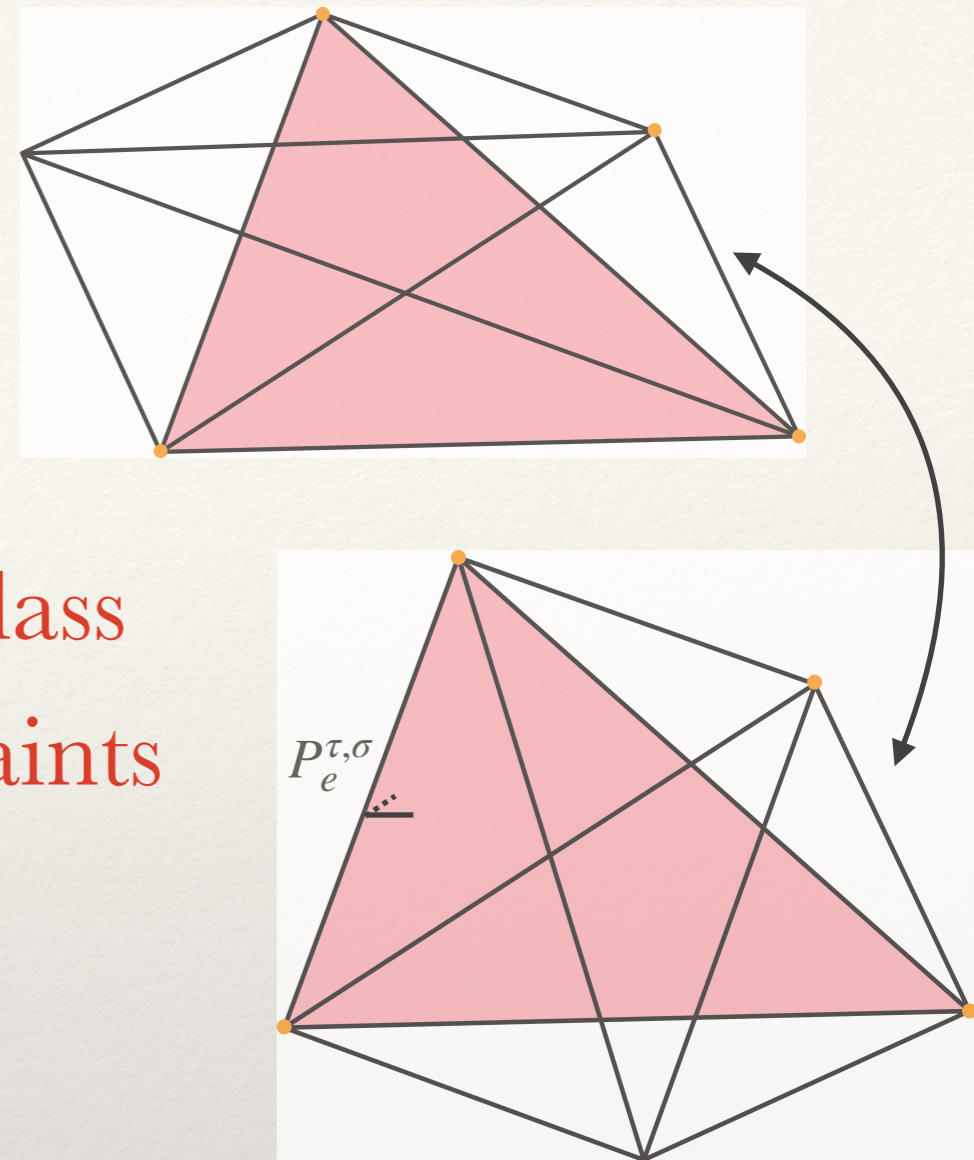
We can localize constraints to a single 4-simplex by introducing the two additional variables $p_{e_i}^\tau$ per τ to our theory and imposing

$$\mathcal{C}_i \equiv p_{e_i}^\tau - P_{e_i}^{\tau,\sigma}(a) = 0, \quad i = 1, 2. \quad \text{2nd class constraints}$$

The advantage of these localized constraints is that they preserve additive factorization of the Regge action and allow us to write the path integral in a product factorized form.

Importantly, as we've seen, dot products at a pair of non-opposite edges (e_1, e_2) do not commute. Instead

$$\{p_{e_1}^\tau, p_{e_2}^\tau\} = \pm \gamma \frac{9}{2} \text{Vol}_\tau^2, \quad \text{with } (e_1, e_2) \text{ non-opposite.}$$



The Area Regge action, $S_{\text{Regge}} = \sum_t a_t \epsilon_t$, factorizes additively. Boundaries of the triangulation Δ are readily included.

From the definition of the deficit angle

$$\epsilon_t = 2\pi - \sum_{\sigma \supset t} \theta_t^\sigma,$$

we see that the area Regge action factorizes

$$S_{\text{ARC}} = \sum_t a_t \epsilon_t = \sum_t n_t \pi a_t - \sum_\sigma \sum_{t \supset \sigma} a_t \theta_t^\sigma(a) \equiv \sum_t S_t^a(a) + \sum_\sigma S_\sigma^a(a).$$

The last equality defines the triangle and simplex actions

$$S_t^a = n_t \pi a_t \quad \text{and} \quad S_\sigma^a(a) = - \sum_{t \supset \sigma} a_t \theta_t^a(L^\sigma(a)).$$

Here the index $n_t \in \{1,2\}$ allows for triangulations with boundary: it is 1 for triangles on the boundary and 2 for triangles in the bulk.

To this action we add a set of functions g that impose the constraints; these act to glue simplices through tetrahedra τ

$$S_{\text{Tot}} = \sum_t S_t^a(a) + \sum_\sigma S_\sigma^a(a) + \sum_{\tau \subset \text{blk}} g_\tau^{\sigma, \sigma'}(a).$$

This constraint discussion was classical, finally we come to our quantum input: the discrete area spectrum found above

$$a(j) = \gamma a_P \sqrt{j(j+1)} \sim \gamma a_P (j + 1/2), \quad \text{with } a_P = 8\pi\hbar G/c^3.$$

(Again j is an half-integer spin label and γ is the area gap.) But, this leads to an important tension...

If we impose the constraints too strongly, there will be no tetrahedra with (half-integer) areas that satisfy them.



We are forced to navigate between Scylla—reducing too much the density of states—and Charybdis—imposing dynamics that does not match GR \rightsquigarrow weak imposition of constraints.

Defining an Effective Spin Foam model

In this context we can define the spin foam

$$\mathcal{Z} = \sum_{\{j_t\}} \mu(j) \prod_t \mathcal{A}_t(j) \prod_\sigma \mathcal{A}_\sigma(j) \prod_{\tau \in \text{blk}} G_\tau^{\sigma, \sigma'}(j),$$

with

$$\mathcal{A}_t = e^{i\gamma n_t \pi(j_t + \frac{1}{2})} \quad \text{and} \quad \mathcal{A}_\sigma = e^{-i\gamma \sum_{t \supset \sigma} (j_t + \frac{1}{2}) \theta_t^\sigma(j)}.$$

In practice, we take $\mu(j) = 1$ for spins satisfying the constraints.

The factors $G_\tau^{\sigma, \sigma'}$ implement the constraints: imposing these sharply, with $G_\tau^{\sigma, \sigma'} = 1$ if satisfied and 0 else, leads to diophantine eqs. for the constraints that will only be satisfied for rare and special labels $\{j_t\}$;

this is the key fact that \rightsquigarrow **weak imposition of the constraints**

We implement the constraints with

$$G_\tau^{\sigma, \sigma'}(j) = \langle \mathcal{K}_\tau(\cdot; P_{e_i}^{\tau, \sigma}(j)) | \mathcal{K}_\tau(\cdot; P_{e_i}^{\tau, \sigma'}(j)) \rangle.$$

**Coherent state
peaked on P 's**

Inputs and Approximations for the Numerics

The spin foam

$$\mathcal{Z} = \sum_{\{j_t\}} \mu(j) \prod_t \mathcal{A}_t(j) \prod_\sigma \mathcal{A}_\sigma(j) \prod_{\tau \in \text{blk}} G_\tau^{\sigma, \sigma'}(j),$$

with $\mu(j) = 1$,

$$\mathcal{A}_t = e^{i\gamma n_t \pi (j_t + \frac{1}{2})} \quad \text{and} \quad \mathcal{A}_\sigma = e^{-i\gamma \sum_{t \supset \sigma} (j_t + \frac{1}{2}) \theta_t^\sigma(j)}.$$

To keep the numerics tractable researchers:

- ▲ consider symmetry reduced triangulations
- ▲ approximate the coherent inner products by real gaussians with widths determined by the $\{\mathcal{C}_i, \mathcal{C}_j\} = \pm \gamma(9/2) \text{Vol}_\tau^2$ non-commutation
- ▲ and consider scaling with both j and γ .

Overview of Results

In quantizing the geometry of 3D/4D triangulations we:

- ▲ use area vectors \vec{A}_τ in τ as $SU(2)/SU(1,1)$ angular momentum operators
- ▲ scale the normals by γ , the area gap (Barbero-Immirzi parameter)
- ▲ leverage closure and global rotations to parametrize tetrahedral geometries by four areas a_τ and two inner products $p_{e_i}^\tau$

Gluing tetrahedra to form a 4-simplex leads to an over parametrization, so we

- ▲ impose constraints to ensure consistent length assignments $\mathcal{C}_i = p_{e_i}^\tau - P_{e_i}^{\tau,\sigma}(a) \stackrel{!}{=} 0$
- ▲ There are two non-commuting constraints \mathcal{C}_i per tetrahedron — second class

Remarks

Uncertainty relations and the area spectrum prevent a sharp imposition of the constraints in the quantum theory

- ▲ In Effective Spin Foams (ESF), we implement constraints weakly, similarly to EPRL-FK

Another approach is to impose constraints classically and quantize the reduced phase space

- ▲ this leads to a phase space with a complicated topology: still an open issue

Effective Spin Foam models

The structure of an effective spin foam can be decomposed into four parts. These models are discrete path integrals for a fixed triangulation Δ with

$$\mathcal{Z}_{\text{ESF}} = \sum_{\{a_t\}} \mu(a) \exp\left(\frac{i}{\hbar} S_{\text{ARC}}(a)\right) \prod_{\sigma} \Theta_{\sigma}^{\text{tr}}(a) \prod_{\tau} G_{\tau}^{\sigma, \sigma'}(a)$$

$\mu(a)$ is the measure term. We anticipate that this can be fixed by demanding invariance under coarse graining or implementing an approximate version of diffeomorphism invariance

$S_{\text{ARC}}(a)$ is the area Regge action and determines the oscillatory part of the partition function

$\Theta_{\sigma}^{\text{tr}}(a)$ implements the generalized triangle inequalities for a 4-simplex

$G_{\tau}^{\sigma, \sigma'}(a)$ implements the constraints between the areas weakly via a Gaussian

ESF can be used to study many features of quantum gravity, such as sum over orientations, causal structures, topology change, etc.

Weak Constraints and the semiclassical regime of the theory

Gluing more simplices, the constraints \mathcal{C}_i will impose further relations between the areas.

Given a 4-simplex σ , the \mathcal{C}_i reduce the 20 variables (a_t, p_e^τ) to 10 areas a_t

$$\mathcal{C}_i = p_{e_i}^\tau - P_{e_i}^{\tau, \sigma}(a) \stackrel{!}{=} 0.$$

For example, if $\tau \subset \sigma \cap \sigma'$, then $p_{e_i}^\tau$ appears both in σ and in σ' , and

$$P_{e_i}^{\tau, \sigma}(a) - P_{e_i}^{\tau, \sigma'}(a) \stackrel{!}{=} 0 \quad (\text{area constraints}).$$

These constraints lead to: consistent lengths; a non-locality (involving pairs of simplices); and can be written in terms of local $p_{e_i}^\tau$ variables.

Discrete area eigenvalues and the constraints lead to diophantine equations with few or no solutions when constraints are imposed strongly.

Hence, we will impose constraints weakly, but as strongly as allowed by the uncertainly relations in order to get good dynamics.

More Details on Implementing the Constraints

In an LQG quantization, the two angle d.o.f. $p_{e_i}^\tau$ are intertwiners

- ▲ There is an $SU(2)$ coherent state construction for the intertwiner space
- ▲ the coherent states $\mathcal{K}_\tau(\cdot, P_{e_i}^{\tau, \sigma}(a))$ are peaked on the $P_{e_i}^{\tau, \sigma}(a)$ ‘angle’ parameters

Gluing two simplifies σ and σ' along a shared tetrahedron τ

- ▲ amounts to integrating two coherent states over τ and gives the inner product

$$G_\tau^{\sigma, \sigma'}(a) \equiv \langle \mathcal{K}_\tau(\cdot, P_i^{\tau, \sigma}(a)) | \mathcal{K}_\tau(\cdot, P_i^{\tau, \sigma'}(a)) \rangle$$

- ▲ gives a function peaked on the constraints $\mathcal{C}_i = P_{e_i}^{\tau, \sigma}(a) - P_{e_i}^{\tau, \sigma'}(a)$

For Effective Spin Foams, we will approximate $G_\tau^{\sigma, \sigma'}$ with a gaussian function

$$G_\tau^{\sigma, \sigma'}(a) = \mathcal{N} \exp\left(-\frac{\mathcal{C}_1^2 + \mathcal{C}_2^2}{4\Sigma^2}\right),$$

Here Σ^2 is the deviation determined by the commutation relations $\Sigma^2 = \ell_P^2 \gamma(9/2) \text{Vol}_\tau^2$.

Weak Constraints

It will be useful to zoom out and consider a simple toy model with weak constraints. This will give a sense of their general behavior:

Consider the oscillatory integral

$$\iint e^{i\lambda S(x,y)} e^{-\mu \mathcal{C}(x,y)^2} dx dy.$$

We impose a constraint \mathcal{C} in both a strong & a weak manner and compute expectation values for $\mathcal{O} = e^{-x^2}$ using

$$\langle \mathcal{O} \rangle_\mu = \frac{\int_{-\infty}^{\infty} \int_{-\infty}^{\infty} \exp(i\lambda(x^2 + y^2)) \exp(-\mu(y - x + 2)^2) \exp(-x^2) dy dx}{\int_{-\infty}^{\infty} \int_{-\infty}^{\infty} \exp(i\lambda(x^2 + y^2)) \exp(-\mu(y - x + 2)^2) dy dx}$$

with $S = x^2 + y^2$ and $\mathcal{C} = y - (x - 2)$.

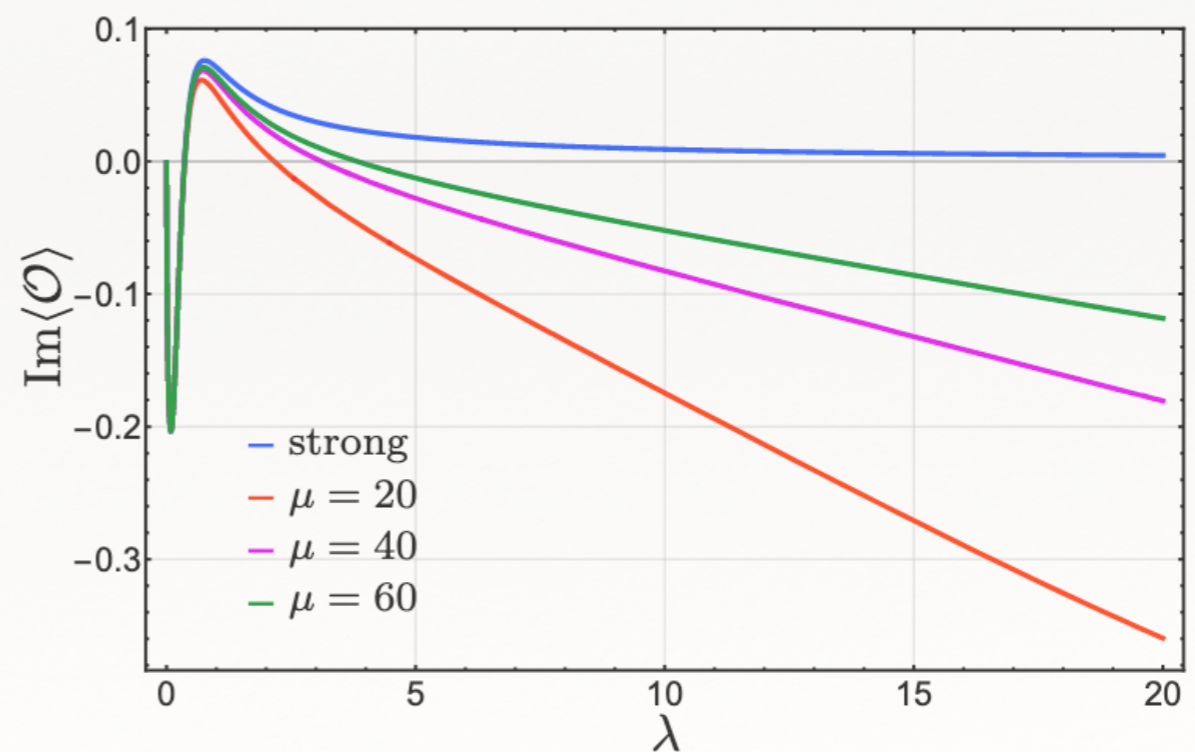
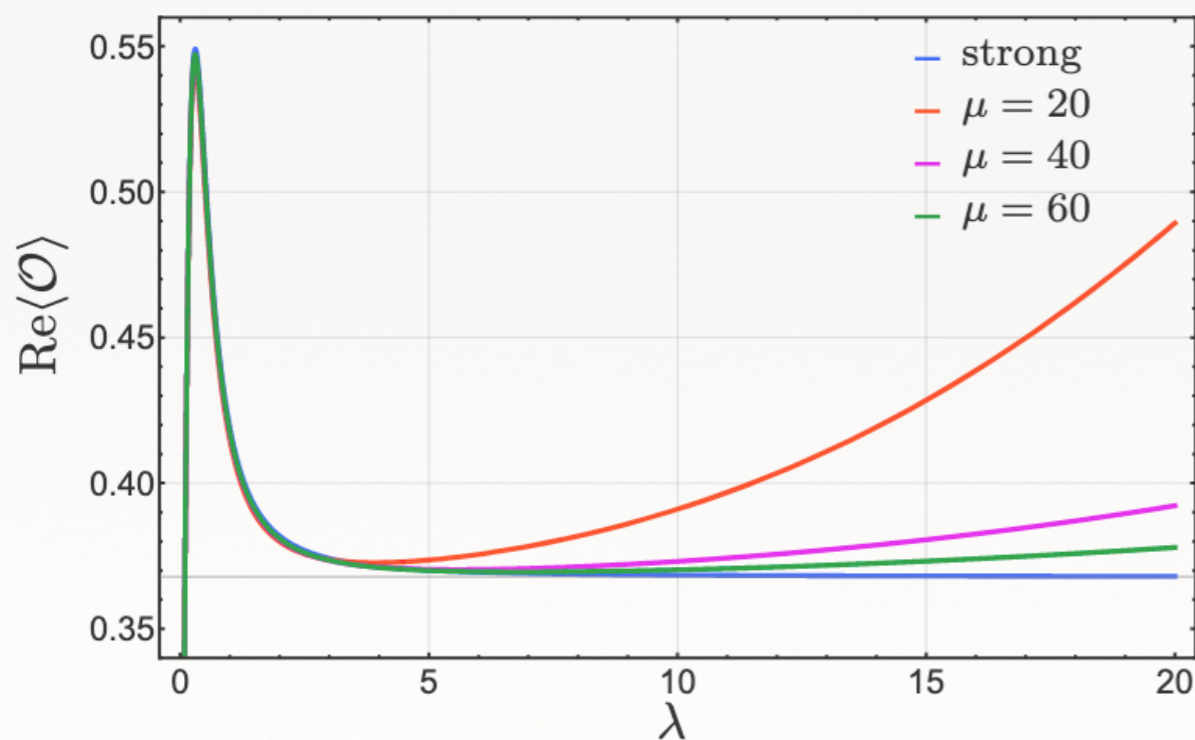
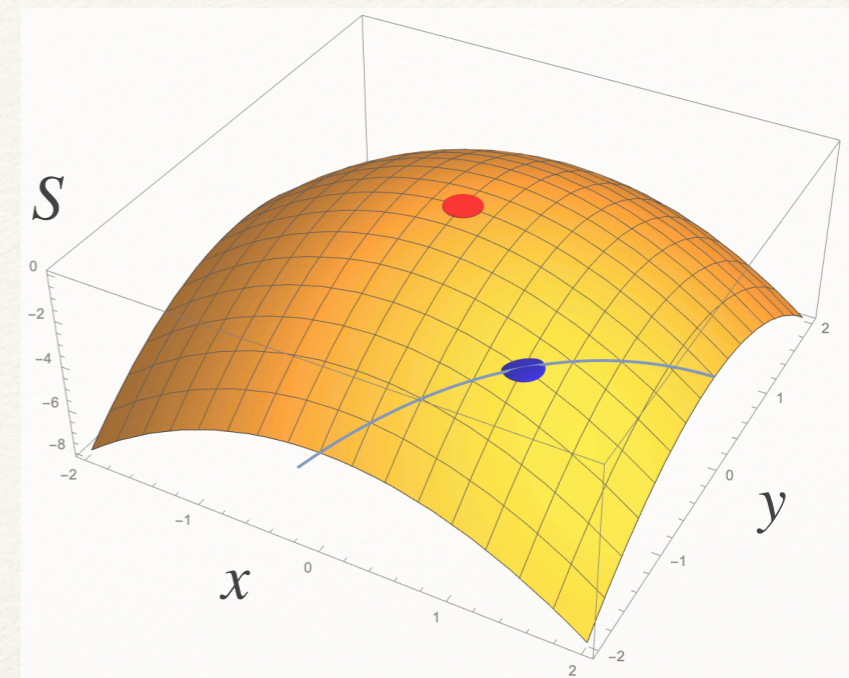
Weak Constraints

Take the oscillatory integral

$$\iint e^{i\lambda S(x,y)} e^{-\mu \mathcal{C}(x,y)^2} dx dy,$$

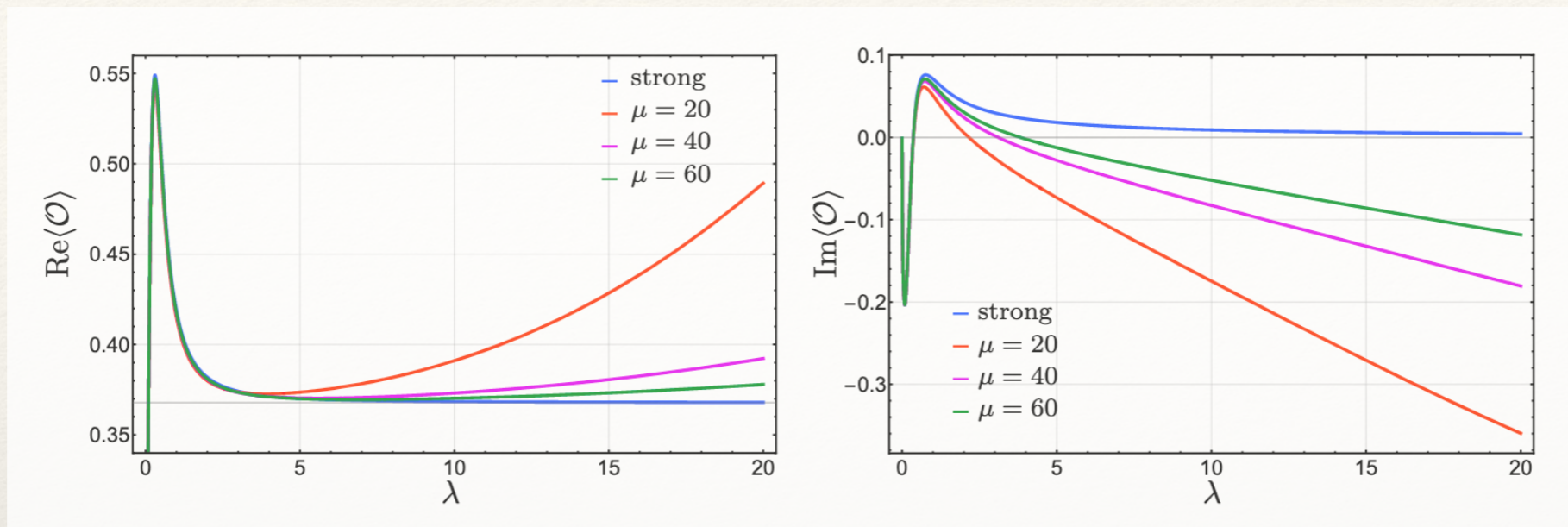
with $S = x^2 + y^2$ and $\mathcal{C} = y - (x - 2)$.

The constrained action $S = x^2 + (x - 2)^2$ has a critical point at $(x, y) = (1, -1)$, and hence the classical expectation value is $\langle \mathcal{O} \rangle_{Cl} = e^{-1} \approx 0.368$. Compare

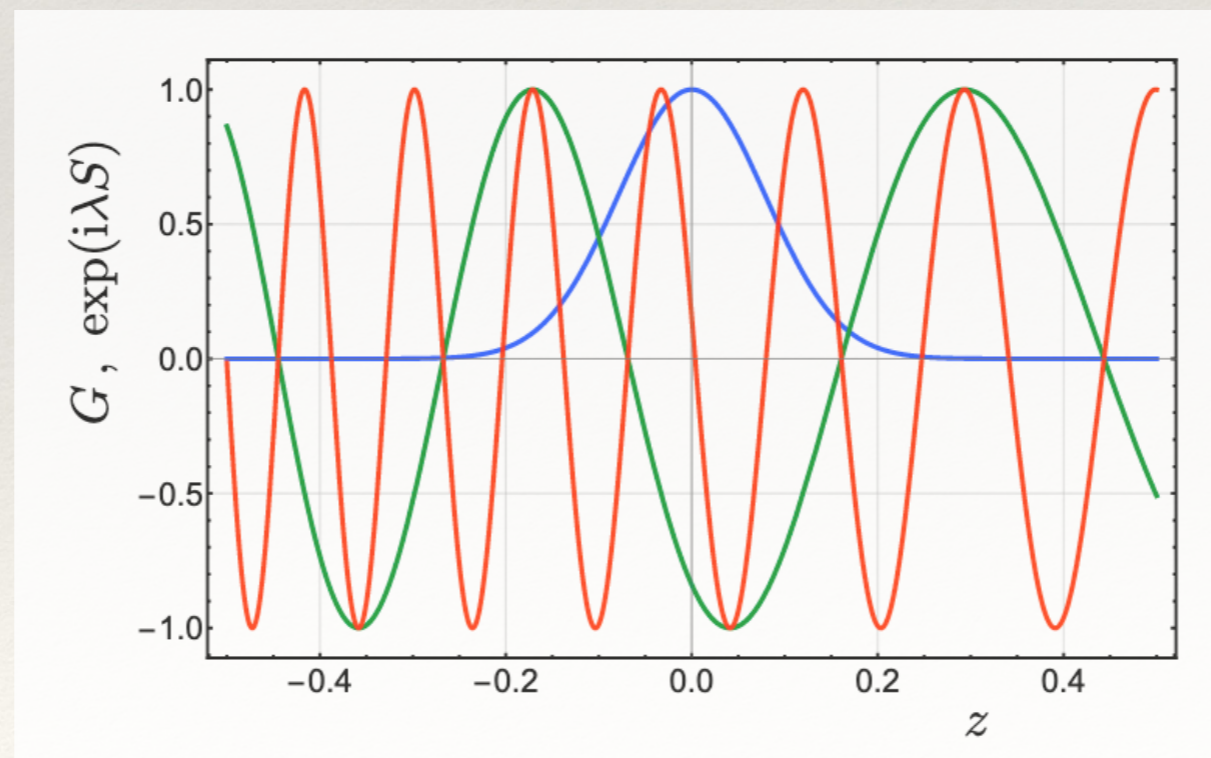


Weak Constraints

Why does the expectation value escape at large λ ?



There is an interplay between the integrand's oscillations and the gaussian constraints:

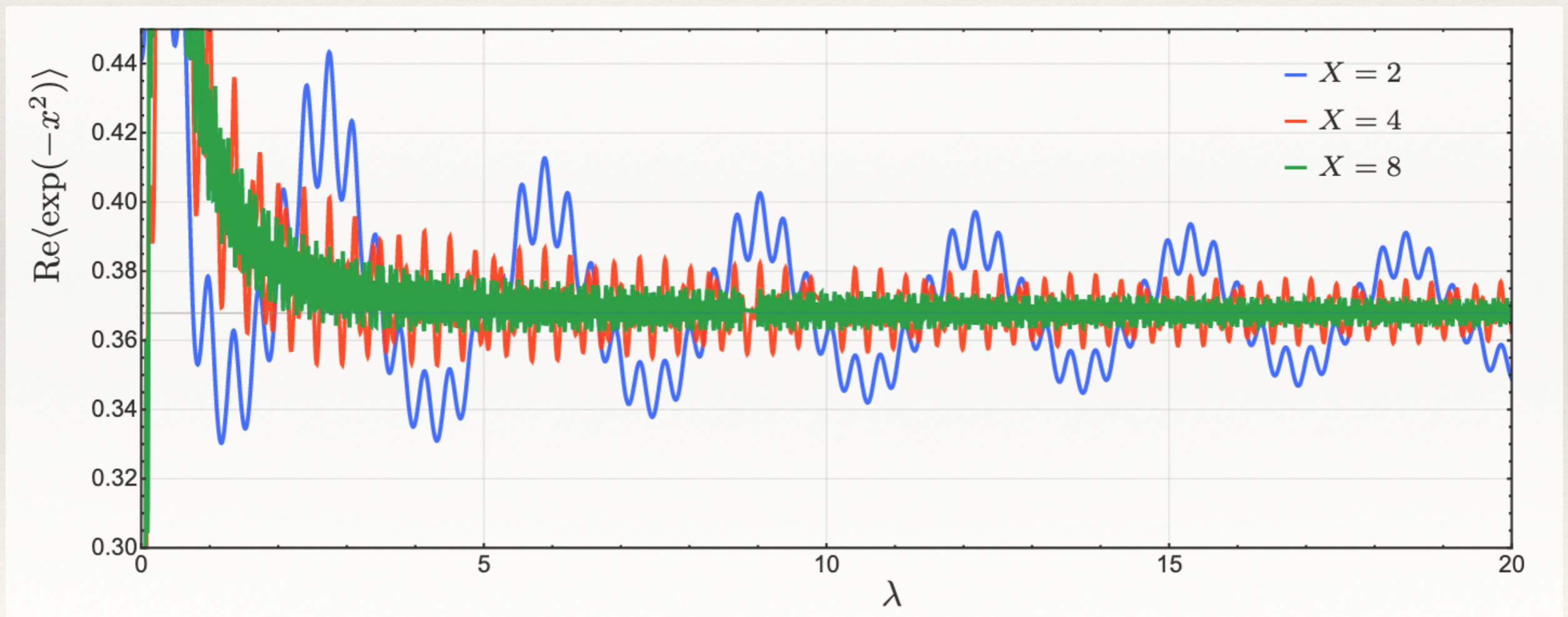


G
 $\lambda = 5$
 $\lambda = 15$

Weak Constraints

We can also investigate truncating the bounds

$$\langle \mathcal{O} \rangle_\mu = \frac{\int_{-X}^X \int_{-X}^X \exp(i\lambda(x^2 + y^2)) \exp(-\mu(y - x + 2)^2) \exp(-x^2) dy dx}{\int_{-X}^X \int_{-X}^X \exp(i\lambda(x^2 + y^2)) \exp(-\mu(y - x + 2)^2) dy dx}$$



Semiclassical Regime

The # of oscillations of the phase factor occurring over the width of the Gaussian (near const. crit. pt.) should be less than a number of order 1.

We turn this into a 1D problem by considering the direction of the steepest change of the constraint $\vec{c} = \vec{\nabla} C / |\vec{\nabla} C|$ and require

gaussian width in \vec{c} direction

$$\lambda \times \left(\left| \vec{\nabla} S \cdot \vec{c} \right| \right) \Big|_{\text{const. crit. pt.}} \times \sigma(\vec{c}) \lesssim \mathcal{O}(1).$$

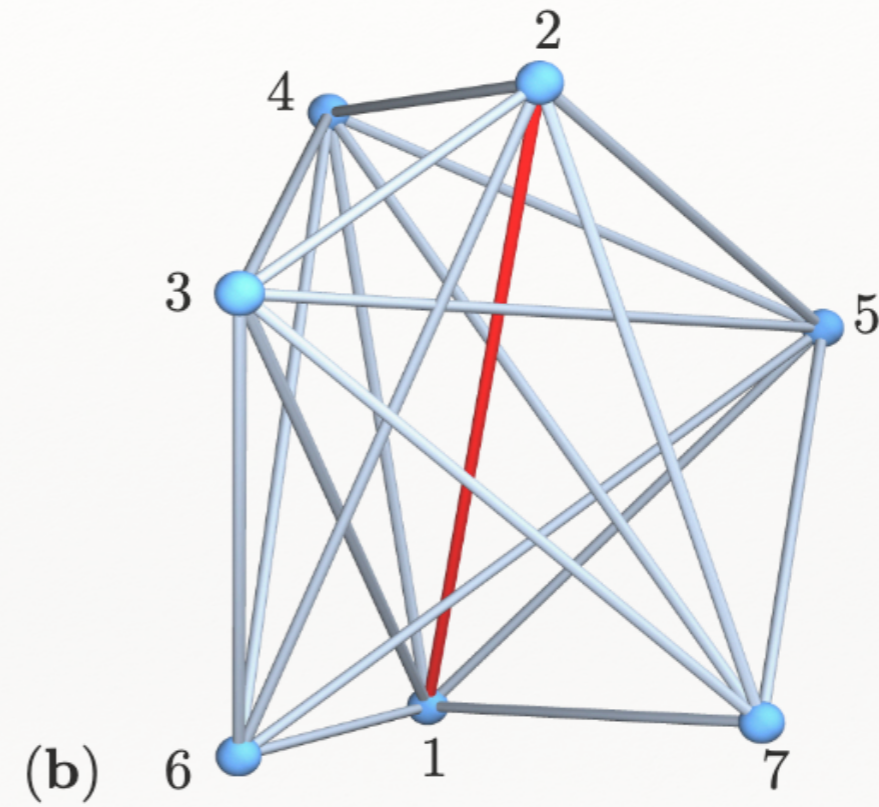
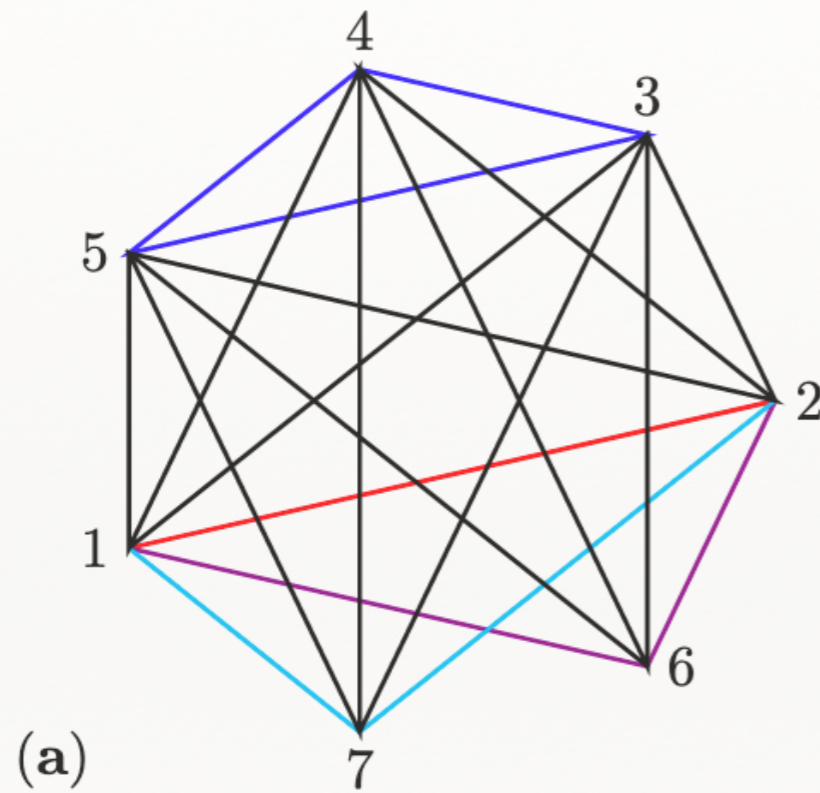
Plugging in these factors for the Effective Spin Foam models gives

$$\frac{\sqrt{\gamma a_t}}{\ell_P} \epsilon_t = \gamma \sqrt{j} \epsilon_t \lesssim \mathcal{O}(1).$$

This formula is the key to understanding the ‘flatness problem’:
the semiclassical regime is *not* just $j \gg 1$!

Numerical Results

I will present results for the following triangulation



Symmetry reduced numerical triangulation:

Δ consists of 6 simplices around one edge

We apply a certain symmetry reduction, so that there are only 3 bndry and 3 bulk areas (4 bndry lengths and 1 bulk length).

There are 3 simplices of type 1 and three simplices of type 2. In each type, all simplices have the same geometry.

The path integral involves 1 bulk variable in LRC and 3 area variables in (constrained) ARC. However, making use of the fall off of the G functions, we can significantly reduce the summation range and gain time savings in the numerics.

Symmetry reduced numerical triangulation:

Δ consists of 6 simplices around one edge

For completeness, here is the definition of this Δ :

vertices:	$m,n=0,1; \quad i,j=2,3,4$	$k=5,5'$
simplices:	$(0,1,2,3,5)$	$(01,2,3,5')$
	$(0,1,2,4,5)$	$(0,1,2,4,5')$
	$(0,1,3,4,5)$	$(0,1,3,4,5')$
lengths:	$l_{01} = t \quad \text{blk}$	$l_{01} = t \quad \text{blk}$
	$l_{mi} = l_{ik} \equiv x$	$l_{mi} = l_{ik} \equiv x$
	$l_{ij} \equiv y$	$l_{ij} \equiv y$
	$l_{m5} \equiv z$	$l_{m5'} \equiv z'$
areas:	$A(x, x, y)$	$A(x, x, y)$
	$A(x, x, t) \quad \text{blk}$	$A(x, x, t) \quad \text{blk}$
	$A(x, x, z)$	$A(x, x, z')$
	$A(z, z, t) \quad \text{blk}$	$A(z', z', t) \quad \text{blk}$

This model illustrates that spin foams can avoid the flatness problem in a range of spin j and Barbero-Immirzi parameter γ

E.g. at $\gamma = 0.1$, for Δ_3 we have

$$\epsilon(A(x, x, t)) = 3.19 - 0.20i, \quad \epsilon(A(z, z, t)) = -1.32 + 0.18i, \text{ and}$$

$$\epsilon(A(z', z', t)) = -0.59 + 0.07i$$

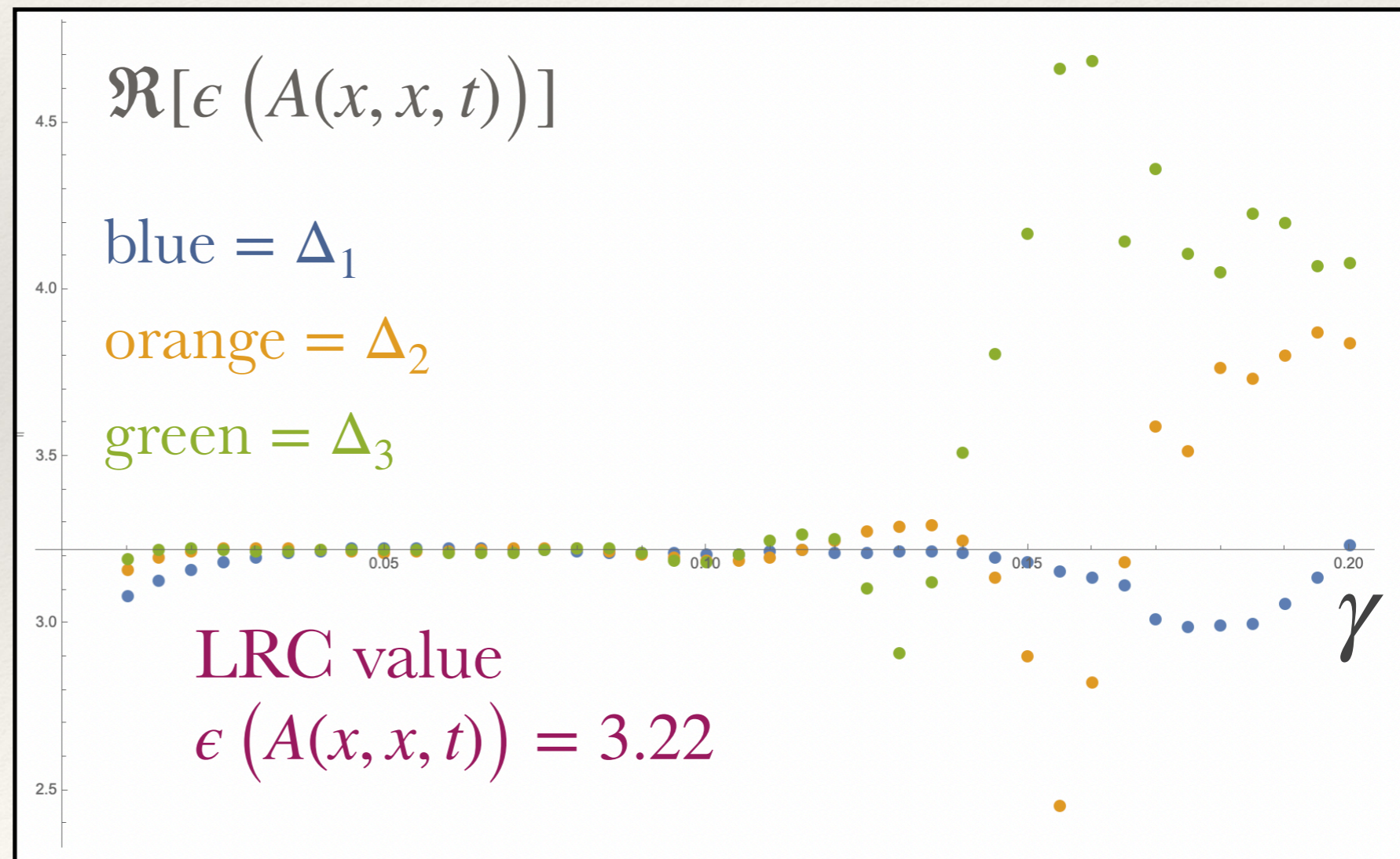
Compare the LRC values:

$$\epsilon(A(x, x, t)) = 3.22$$

$$\epsilon(A(z, z, t)) = -1.36$$

and

$$\epsilon(A(z', z', t)) = -0.607$$



Effective Spin Foam models

The structure of an effective spin foam can be decomposed into four parts. These models are discrete path integrals for a fixed triangulation Δ with

$$\mathcal{Z}_{\text{ESF}} = \sum_{\{a_t\}} \mu(a) \exp\left(\frac{i}{\hbar} S_{\text{ARC}}(a)\right) \prod_{\sigma} \Theta_{\sigma}^{\text{tr}}(a) \prod_{\tau} G_{\tau}^{\sigma, \sigma'}(a)$$

$\mu(a)$ is the measure term. We anticipate that this can be fixed by demanding invariance under coarse graining or implementing an approximate version of diffeomorphism invariance

$S_{\text{ARC}}(a)$ is the area Regge action and determines the oscillatory part of the partition function

$\Theta_{\sigma}^{\text{tr}}(a)$ implements the generalized triangle inequalities for a 4-simplex

$G_{\tau}^{\sigma, \sigma'}(a)$ implements the constraints between the areas weakly via a Gaussian

ESF can be used to study many features of quantum gravity, such as sum over orientations, causal structures, topology change, etc.

Thank you!

My son, Milo, doing calculations in 2013...



...and studying
Jimmy in 2022

I am hugely grateful to the Quantum Information Structure of Spacetime (QISS) Project and to the Perimeter Institute for Theoretical Physics for their support of my work.

My work on these lectures was made possible through the support of the ID# 62312 grant from the John Templeton Foundation, as part of the 'The Quantum Information Structure of Spacetime' Project (QISS). The opinions expressed in this project/publication are those of the author and do not necessarily reflect the views of the John Templeton Foundation.

Research at Perimeter Institute is supported in part by the Government of Canada through the Department of Innovation, Science and Economic Development Canada and by the Province of Ontario through the Ministry of Colleges and Universities.